



**Intel® Model: 18260NGW, FCC ID:
PD918260NG**

Intel model 18260NGW embedded inside Lenovo model TP00076B

RF Exposure Power Density and Evaluation Test Report

July 2016

Revision 1.5



Notice: This document contains information on products in the design phase of development. The information here is subject to change without notice. Do not finalize a design with this information.

INFORMATION IN THIS DOCUMENT IS PROVIDED IN CONNECTION WITH INTEL PRODUCTS. NO LICENSE, EXPRESS OR IMPLIED, BY ESTOPPEL OR OTHERWISE, TO ANY INTELLECTUAL PROPERTY RIGHTS IS GRANTED BY THIS DOCUMENT. EXCEPT AS PROVIDED IN INTEL'S TERMS AND CONDITIONS OF SALE FOR SUCH PRODUCTS, INTEL ASSUMES NO LIABILITY WHATSOEVER AND INTEL DISCLAIMS ANY EXPRESS OR IMPLIED WARRANTY, RELATING TO SALE AND/OR USE OF INTEL PRODUCTS INCLUDING LIABILITY OR WARRANTIES RELATING TO FITNESS FOR A PARTICULAR PURPOSE, MERCHANTABILITY, OR INFRINGEMENT OF ANY PATENT, COPYRIGHT OR OTHER INTELLECTUAL PROPERTY RIGHT.

A "Mission Critical Application" is any application in which failure of the Intel Product could result, directly or indirectly, in personal injury or death. SHOULD YOU PURCHASE OR USE INTEL'S PRODUCTS FOR ANY SUCH MISSION CRITICAL APPLICATION, YOU SHALL INDEMNIFY AND HOLD INTEL AND ITS SUBSIDIARIES, SUBCONTRACTORS AND AFFILIATES, AND THE DIRECTORS, OFFICERS, AND EMPLOYEES OF EACH, HARMLESS AGAINST ALL CLAIMS COSTS, DAMAGES, AND EXPENSES AND REASONABLE ATTORNEYS' FEES ARISING OUT OF, DIRECTLY OR INDIRECTLY, ANY CLAIM OF PRODUCT LIABILITY, PERSONAL INJURY, OR DEATH ARISING IN ANY WAY OUT OF SUCH MISSION CRITICAL APPLICATION, WHETHER OR NOT INTEL OR ITS SUBCONTRACTOR WAS NEGLIGENT IN THE DESIGN, MANUFACTURE, OR WARNING OF THE INTEL PRODUCT OR ANY OF ITS PARTS.

Intel may make changes to specifications and product descriptions at any time, without notice. Designers must not rely on the absence or characteristics of any features or instructions marked "reserved" or "undefined." Intel reserves these for future definition and shall have no responsibility whatsoever for conflicts or incompatibilities arising from future changes to them. The information here is subject to change without notice. Do not finalize a design with this information.

Intel software products are copyrighted by and shall remain the property of Intel Corporation. Use, duplication, or disclosure is subject to restrictions stated in Intel's Software License Agreement, or in the case of software delivered to the government, in accordance with the software license agreement as defined in FAR 52.227-7013.

The products described in this document may contain design defects or errors known as errata which may cause the product to deviate from published specifications. Current characterized errata are available on request.

The code names presented in this document are only for use by Intel to identify products, technologies, or services in development that have not been made commercially available to the public, i.e., announced, launched, or shipped. They are not "commercial" names for products or services and are not intended to function as trademarks.

Contact your local Intel sales office or your distributor to obtain the latest specifications and before placing your product order.

Copies of documents which have an order number and are referenced in this document, or other Intel literature may be obtained by calling 1-800-548-4725 or by visiting Intel's website at <http://www.intel.com/design/literature.htm>.

Intel processor numbers are not a measure of performance. Processor numbers differentiate features within each processor family, not across different processor families. See http://www.intel.com/products/processor_number for details.

Intel is a trademark of Intel Corporation or in the US and other countries.

* Other brands and names may be claimed as the property of others.

Copyright © 2015 Intel Corporation. All rights reserved.



Table of Contents

| | | |
|----------|--|-----------|
| 1 | Document Scope | 7 |
| 2 | Background – WiGig System Operation | 8 |
| 2.1 | System Block Diagram | 8 |
| 2.2 | Beam Forming..... | 9 |
| 2.3 | TX Duty Cycle | 9 |
| 2.4 | Intel 18260NGW Module in Lenovo Model TP00076B | 9 |
| 3 | Simulation Methodology | 10 |
| 3.1 | Assessment considerations | 10 |
| 3.2 | Near field & transition-zone field results | 10 |
| 3.3 | Simulation tool..... | 10 |
| 3.3.1 | Tool description | 10 |
| 3.3.2 | Solver description | 10 |
| 3.3.3 | Convergence criteria and Power Density Calculations..... | 11 |
| 3.4 | Finding near field worst case simulation configuration | 12 |
| 3.4.1 | Terminology:..... | 13 |
| 3.4.2 | Primer on field vector representation: | 13 |
| 3.4.3 | Domain search for worst case direction..... | 15 |
| 3.5 | 3D Models Used in the Simulation..... | 17 |
| 3.5.1 | Worst case operating conditions of the platform..... | 17 |
| 3.5.2 | RFEM 2 housing inside Intel 18260NGW module | 18 |
| 3.5.3 | Closest distance to the body of an end user | 19 |
| 3.5.4 | Metals in proximity of the RFEM 2 | 19 |
| 3.6 | Antenna feed | 20 |
| 4 | Simulation Results | 21 |
| 4.1 | Results on the Edge area | 22 |
| 4.1.1 | Upper bound simulation results for edge plane exposure..... | 22 |
| 4.1.2 | Single-point power density values with worst-case antenna phases for edge plane exposure | 25 |
| 4.1.3 | One dimensional cut of the mesh single-point power density for edge plane exposure | 28 |
| 4.1.4 | Integrated power density over 1 cm ² for edge plane exposure | 29 |
| 4.1.5 | Power density for edge plane exposure..... | 30 |
| 4.2 | Results on the Base area. | 35 |
| 4.2.1 | Upper bound simulation results for base plane exposure | 35 |
| 4.2.2 | Single-point power density values with worst case antenna phases for base plane exposure | 38 |
| 4.2.3 | One dimensional cut of the mesh single-point power density for base plane exposure | 41 |
| 4.2.4 | Integrated power density over 1 cm ² for base plane exposure | 42 |
| 4.2.5 | Power density for base plane exposure | 45 |
| 4.3 | Conclusion | 48 |
| 5 | Validation of Simulation Model in Transition-Zone Field to Far-Field | 49 |
| 5.1 | Correlation of E.I.R.P. in the near to far field..... | 49 |
| 5.1.1 | Far field boundary calculation | 49 |
| 5.1.2 | Test laboratory | 50 |
| 5.1.3 | Correlation of measurements and simulation | 50 |
| 5.1.4 | Estimated conducted power level | 53 |
| 5.2 | Simulating a canonical antenna design | 54 |
| 6 | Summary | 57 |



List of Figures

| | |
|--|----|
| Figure 1 – Intel 18260NGW module system block diagram | 8 |
| Figure 2 – Illustration of the Adaptive Mesh Technique | 11 |
| Figure 3 – Search Planes are the x-y planes (i.e. the transparent plane as illustrated in this picture- Left: Base plane Right: Edge plane) | 12 |
| Figure 4 – Near field worst case terminology and orientation | 13 |
| Figure 5 - Platform operating modes | 17 |
| Figure 6 - Platform worst case operating mode | 17 |
| Figure 7 – Active antenna inside the platform | 18 |
| Figure 8 – Simulated area on the base..... | 19 |
| Figure 9 – Simulated area on the edge | 19 |
| Figure 10 – Edge plane illustration | 22 |
| Figure 11 – Channel 1 upper bound, Single-point Power Density mesh on platform edge | 23 |
| Figure 12 – Channel 2 upper bound, Single-point Power Density mesh on platform edge | 23 |
| Figure 13 – Channel 3 upper bound, Single-point Power Density mesh on platform edge | 24 |
| Figure 14 – Footprint of single-point power density plane representation in edge plane..... | 24 |
| Figure 15 – Channel 1 single-point power density mesh on platform edge | 26 |
| Figure 16 – Channel 2 single-point power density mesh on platform edge | 27 |
| Figure 17 – Channel 3 single-point power density mesh on platform edge..... | 27 |
| Figure 18 – One dimensional plots of the power density on Channel 1 | 28 |
| Figure 19 – One dimensional plots of the power density on Channel 2 | 28 |
| Figure 20 – One dimensional plots of the power density on Channel 3 | 28 |
| Figure 21 – Channel 1 worst case - Integrated power over 1cm ² an platform edge | 29 |
| Figure 22 – Channel 2 worst case - Integrated power over 1cm ² an platform edge | 29 |
| Figure 23 – Channel 3 worst case - Integrated power over 1cm ² an platform edge | 30 |
| Figure 24 – Footprint of integrated power density plane representation in edge plane..... | 30 |
| Figure 25 – HFSS Simulation results in Ch1 (Edge plane) | 31 |
| Figure 26 – HFSS Simulation results in Ch2 (Edge plane) | 32 |
| Figure 27 – HFSS Simulation results in Ch3 (Edge plane) | 33 |
| Figure 28 –Base plane illustration | 35 |
| Figure 29 – Channel 1 upper bound, Single-point Power Density mesh on platform base..... | 36 |
| Figure 30 – Channel 2 upper bound, Single-point Power Density mesh on platform base..... | 36 |
| Figure 31 – Channel 3 upper bound, Single-point Power Density mesh on platform base..... | 37 |
| Figure 32 – Footprint of single-point power density plane representation in base plane..... | 37 |
| Figure 33 – Channel 1 single-point power density mesh on platform boundary | 40 |
| Figure 34 – Channel 2 single-point power density mesh on platform boundary | 40 |
| Figure 35 – Channel 3 single-point power density mesh on platform boundary | 41 |
| Figure 36 – One dimensional plots of the power density on Channel 1 | 41 |
| Figure 37 – One dimensional plots of the power density on Channel 2 | 42 |
| Figure 38 – One dimensional plots of the power density on Channel 3 | 42 |
| Figure 39 – Channel 1 worst case - Integrated power over 1cm ² on platform base | 43 |
| Figure 40 – Channel 2 worst case - Integrated power over 1cm ² on platform base | 43 |
| Figure 41 – Channel 3 Worst case - Integrated power over 1cm ² on platform base..... | 44 |
| Figure 42 – HFSS Simulation results in Ch1 (Base Plane) | 45 |
| Figure 43 – HFSS Simulation results in Ch2 (Base Plane) | 46 |
| Figure 44 – HFSS Simulation results in Ch3 (Base Plane) | 47 |
| Figure 45 – Antenna Dimensions in mm | 49 |
| Figure 46 – Comparison of E.I.R.P. simulation to lab measurements – channel 1 | 50 |
| Figure 47 – Comparison of E.I.R.P. simulation to lab measurements – channel 2 | 51 |
| Figure 48 – Comparison of E.I.R.P. simulation to lab measurements – channel 3 | 52 |
| Figure 49 – Estimate conducted power from E.I.R.P. data | 53 |



Document Scope

| | |
|--|----|
| Figure 50 – Simulation of a single Patch antenna | 54 |
| Figure 51 – Patch Antenna Gain | 54 |
| Figure 52 – Simulation 3D structure | 55 |
| Figure 53 – Power Density of Canonical Patch Antenna | 56 |

List of Tables

| | |
|---|----|
| Table 1 – Acronyms..... | 6 |
| Table 2 – Phases configurations for the worst case..... | 25 |
| Table 3 – Ratios between Z-power density and total power density on edge area | 26 |
| Table 4 – Worst case power density - Edge plane..... | 33 |
| Table 5 – Edge plane integrated power density at zero distance..... | 34 |
| Table 6 – Phases configurations for the worst case..... | 38 |
| Table 7 – Ratios between Z-power density and total power density on base area | 39 |
| Table 8 – Worst case power density - Base plane | 47 |
| Table 9 – Base plane integrated power density at zero distance | 48 |
| Table 10 – Gain calculation from power density per several distances..... | 55 |
| Table 11 – Summary of simulation results for RF exposure compliance | 57 |



Table 1 – Acronyms

| | |
|----------|--|
| ABS | Acrylonitrile butadiene styrene – the plastic type from which the HP model HSTNN-I22C is built |
| Ant | Antenna |
| Az | Azimuth |
| BB | Base Band |
| BF | Beam Forming |
| BT | Bluetooth |
| BW | Band Width |
| CAD | Computer Aided Design |
| CPU | Central Processing Unit |
| E.I.R.P. | Equivalent Isotropically Radiated Power |
| EI | Elevation |
| EM | Electro-Magnetic |
| GHz | Giga Hertz (109 Hz) |
| IF | Intermediate Frequency |
| MAC | Media Access Control |
| M.2 | M2: Formerly known as Next Generation Form Factor (NGFF); used as specification for connectors of the expansions cards mounted on computer |
| mmWave | Milli-Meter Wave |
| OTP | One Time Programmable memory |
| PC | Personal Computer |
| R&D | Research and Development |
| RF | Radio Frequency |
| RFEM 2 | Radio Front End Module |
| RFIC | Radio Frequency Integrated Circuit |
| RX | Receive |
| SKU | Stock Keeping Unit, specific product model version |
| TPC | Transmit Power Control |
| T/R SW | Transmit / Receive Switch |
| TX | Transmit |
| WiGig | Wireless Gigabit Alliance – the alliance that promoted the 60GHz into 802.11ad standard. |



1 Document Scope

This report is submitted to support the compliance to FCC rule parts §2.1093 and §15.255(g), of Intel 18260NGW WiGig module (FCC ID: PD918260NG), including an active antenna array, embedded inside the Lenovo Model TP00076B platform.

Please note, Lenovo model TP00076B is the regulatory model number. This identical host is also marketed under the name ThinkPad X1 Yoga (Raven). In the report we refer only to TP00076B model.

Per the location of the active antenna array (a.k.a. RFEM 2) in the Lenovo model TP00076B platform, the distance between the antenna array to the body of an end user, at the closest contact point, will be in the near field. At this time power density measurements are not possible.

Therefore, to obtain an estimation of the near field power density results, we used an EM simulation that includes the RFEM 2 transmitter model, embedded inside the Lenovo model TP00076B. The simulation method and the simulation results are described in this document.

Due to the lack of standardized code validation, benchmarking and uncertainty of the simulation software, the near field¹ to far field results are included for the purpose of providing confidence for the software simulation model used and that the results produced were within an acceptable range when compared with the measured results. The error margins of all test results have been considered collectively by the FCC to determine compliance.

To prove the validity of these results, this report shows how the results of the same simulation are correlated to lab measurements for transition-zone field² to far field distances.

The 2nd chapter provides relevant background on Intel 18260NGW module. The 3rd chapter describes the simulation methodology to determine RF exposure (power density) levels. The 4th chapter includes simulation results, and 5th chapter the correlation between simulation and lab measurements in transition-zone field to far field^{3,4}. Chapter 6 summarizes the RF-Exposure analysis.

Please note that this document covers non confidential parts information, relevant details and explanations that qualify for confidentiality are included separately in the test report document entitled "Intel model 18260NGW embedded inside Lenovo model TP00076B - WiGig subsystem theory of operation Revision 1.1"; therefore, not included in the this reports. However, in this document some places make cross-reference to the confidential Operational Description exhibit for details about device operation.

¹ The "near field" nomination is used to indicate the reactive near field zone at antenna proximity particularly the field in the exposure plane. In this report it is the zone between 0 and 5 cm.

² The transition-zone field nomination is used to indicate the radiative near field zone in which the correlation between the measurement and simulation is performed i.e, it is the zone between 5cm and 10 cm

³ The Far field zone nomination is used to indicate the zone above 10cm from the antenna.

⁴ The far field lower distance (10 cm) is determined according to the RFEM 2 dimension. The transition-zone field is the zone going from the lower limit of the measurement distance (5 cm) to the far field lower limit (10 cm).

2 Background – WiGig System Operation

2.1 System Block Diagram

Intel 18260NGW module (FCC ID: PD918260NG) is a solution for embedded WiGig connectivity for various PC client platforms. For this RF exposure evaluation the Intel 18260NGW module will be incorporated into the Lenovo model TP00076B PC. The Lenovo TP00076B is a 2 in 1 PC that can be used in traditional portable laptop notebook mode or converted to a tablet PC (non-detachable) mode.

The client solution for Lenovo TP00076B includes the 18260NGW WiGig module (FCC ID: PD918260NG) connected to a beamforming antenna array RFEM 2 using one IF coaxial cable.

The WiGig module (FCC ID: PD918260NG) is a PCIe M.2 module consisting of a WiGig BB chip, which implements the WiGig MAC, Modem, BF algorithm, and active antenna array module control, as well as the BB + IF stage circuitry. This WiGig module re-uses the same WiGig MAC/BB silicon core as the previous generation module 17265NGW (FCC ID: PD917265NG).

RFEM 2 (10042RRFW) is an active antenna array module, which converts the IF signal to 60GHz signal. It also performs the beamforming functionality by phase shifting the RF signal that goes to each antenna. The RFEM 2 is slave to the WiGig BB chip since all module control and algorithms run on the BB chip.

Intel System-on-Chip (SoC) houses the CPU (central processing unit) which executes different applications, as well as provides the command and control of the client solution, including all I/O data and addressing.

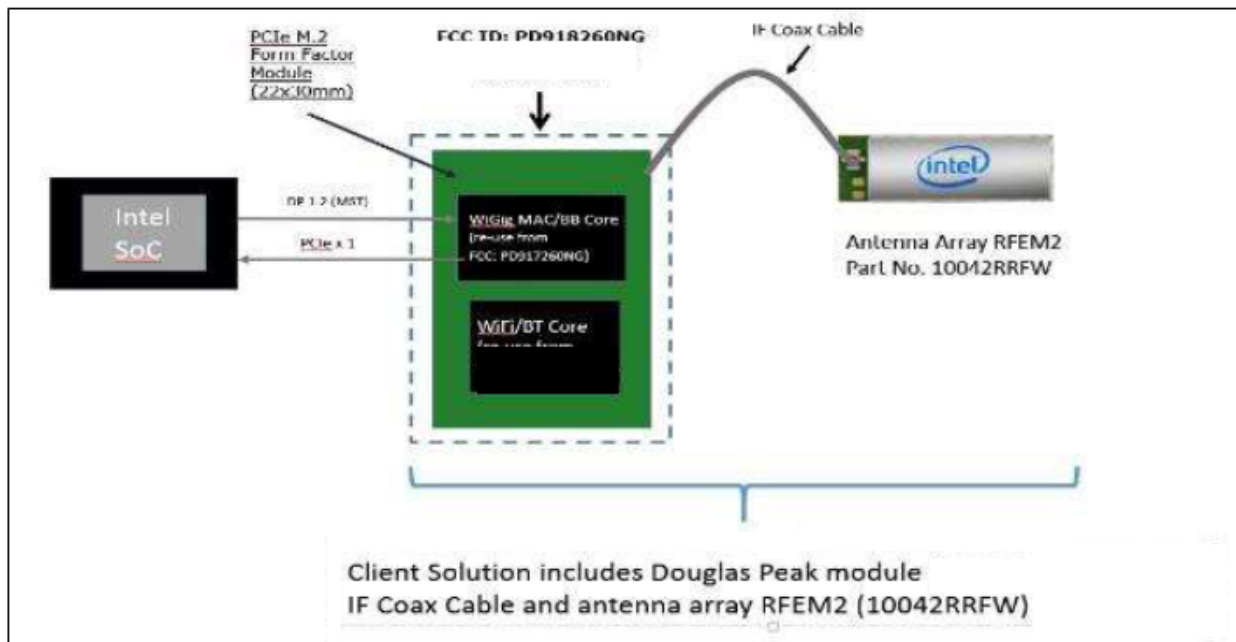


Figure 1 – Intel 18260NGW module system block diagram

In typical application the RFEM 2 is located at the top of the lid of the platform, in order to improve the RF propagation of the communication link



2.2 Beam Forming

Achieving high bandwidth communication over 60GHz channels usually requires directional antenna at the transmitter and receiver sides. In consumer electronics, fixed directional or mechanically rotated antenna are not practical and electronically steerable antenna are usually used.

In Intel 18260NGW module, such electronic steerable antenna array is being used. Beam forming protocol (defined in the standard ISO/IEC/IEEE 8802-11:2012/Amd.3:2014(E), Clause 21) is used to find the right direction for setting both the RX and TX antenna directions.

Due to the RFEM 2 structure it is not easy to predict the direction and beam forming combination that yields the maximum energy in near field. To find this value a search over the possible beam forming combination was made and the worst case value was taken. Detailed explanation of this process can be found in section 0.

2.3 TX Duty Cycle

The WiGig protocol, as defined in ISO/IEC/IEEE 8802-11:2012/Amd.3:2014(E), Clause 21, is packet based with time division multiplexing (TDM). Intel 18260NGW module is configured to guarantee that the TX-Duty-Cycle, defined as the ratio of the duration of all transmissions to the total time, is at most 70% over any 10 seconds period. This was established by worst case analysis, as derived from full system simulation, and verified by measurements.

The limited TX-Duty-Cycle is established based on HW and FW implementation with ~100 ms (102.4 ms) measurement duration and 10 seconds averaging; other details are provided in the Operational Description exhibit. The 70% duty cycle limitation is guaranteed independent of user activity, and therefore it adheres to the source-based time-averaging definition in 2.1093(d)(5).

In addition, measurements of the Intel 18260NGW module configured to obtain maximal TX-Duty-Cycle in a fully loaded system, resulted in actual maximum TX-Duty-Cycle of 58% over any 10 seconds period, lower than the upper bound derived from the analysis in this section.

2.4 Intel 18260NGW Module in Lenovo Model TP00076B

Intel produces several HW SKUs (variations) of Intel 18260NGW module, which target different types of customer platform products.

Lenovo uses Intel 18260NGW module inside the Lenovo Model TP00076B platform. This SKU is characterized by:

1. supporting channels **1+2+3**
2. Reduced power emission, which translates to:
 - a. Maximum transmit conducted power of **6.0 dBm** aggregated conducted power at the antenna ports.
 - b. Maximum TX duty-cycle of **70%**.
3. Antenna array RFEM 2 (100042RRFW).
4. Note that antenna array RFEM 1 (100041RRFW) was also approved as part of the module original approval but is not being implemented with the Lenovo TP00076B. No other antennas have been approved by original or permissive change filings.



3 Simulation Methodology

3.1 Assessment considerations

During the system operation mode it is challenging to define a practical system worst case scenario in which the user is exposed to the highest emission level. To ensure coverage of the highest emission the analysis of the worst case corner condition is used and is emphasized in the following:

1. Platform orientation with respect to human body – in most of the cases when the platform is very close to the human body and the energy is directed to the human body, the human body will attenuate the signal. In this case a reliable link can't be achieved, when a reliable link can't be maintained the system enters search mode. In search mode the system will transmit a low duty cycle of less than 1%. This search mode contains signals which happen every 100ms at the maximum output power.
However – in the analysis done in this document system is simulated in operational mode (not in search mode) operating at 70% duty cycle which is much higher than the search mode.
2. Energy direction, beam forming – In order to avoid human body attenuation or object blockage of a reliable link the system beam forming will automatically search for a path that will establish a more reliable link. So, in real life, in most of the cases the EM path will not be directed towards the human body. However – in the analysis presented in this document worst case beam forming direction is used.

Please note; the above worst case assessment description is very conservative in that it is very unlikely this case would happen under normal usage conditions. Since we cannot state with 100% certainty that this is impossible we kept this worst case assessment methodology, we ask that this is taken into consideration.

3.2 Near field & transition-zone field results

Finding the worst case emission in near field across platform boundary requires searching on two orthogonal domains. One domain is the location – need to find the place that has the worst case energy. The other domain that has to be searched is the antenna phases – need to search over the various antenna phases and find the antenna phase combination that gives the worst case value. Section 3.4 below explains how these two worst cases (location and phase) searches are investigated.

After the completion of the worst case phase analysis, the phases found during this analysis are used to find the worst case integrated energy across 1cm² averaging area for RF exposure evaluation purposes. EM simulation is used for this analysis.

Transition-zone field to far field analysis is both simulated and correlated against measured lab results.

3.3 Simulation tool

3.3.1 Tool description

For the EM simulation the commercially available ANSYS Electronics Desktop 2015 (HFSS) is used. The ANSYS HFSS tool is used in industry for simulating 3-D full-wave electromagnetic fields. Intel uses this EM simulation tool due to its' gold-standard accuracy, advanced solver and high-performance computing technology capabilities for doing accurate and rapid design of high-frequency components.

3.3.2 Solver description

The HFSS simulation is done using the Finite Element Method which operates in the frequency domain. The HFSS is based on an accurate direct solver with first order basis functions.

3.3.3 Convergence criteria and Power Density Calculations

The HFSS uses volume air box containing the simulated area to calculate the EM fields. The box is truncated by PML (Perfect Match Layer) boundary condition. The simulation uses adaptive mesh technique (see below [Figure 2](#)) to meet the exit criteria of $\Delta S < 0.02$. The ΔS is the change in the magnitude of the S-parameters between two consecutive passes, if the magnitude and phase of all S-parameters change by an amount less than the Maximum Delta S per Pass value from one iteration to the next, the adaptive analysis stops.

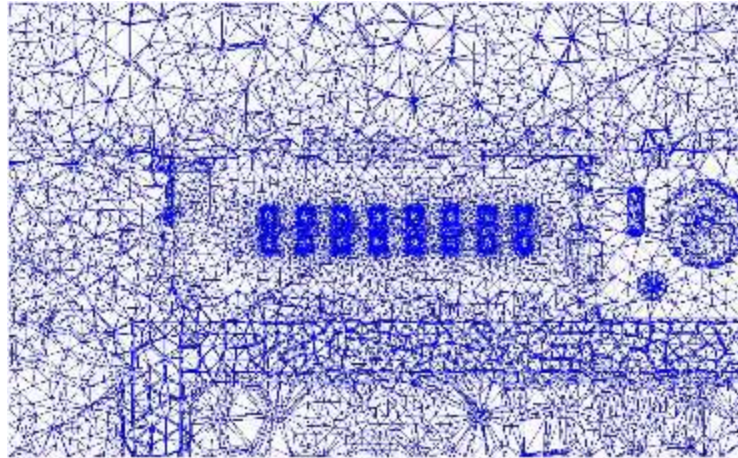


Figure 2 – Illustration of the Adaptive Mesh Technique

After having the simulated electrical and magnetic (E & H) fields in each point in the mesh, the poynting vector is calculated. The integrated power density on a given surface is calculated as the surface integral of the Poynting vector:

$$W = \frac{1}{2} \operatorname{Re} \int_S (\vec{E} \times \vec{H}^*) \cdot \vec{n} dS$$

Note: HFSS phasors in field calculator are peak phasors which leads to the $1/2$ factor in the Poynting vector calculation.



3.4 Finding near field worst case simulation configuration

As explained previously near field analysis requires finding worst case location (along the searched planes) and antenna phase values. As further explained the search should be done on two domains:

- 1) Look for the worst case position (across the search plane).
- 2) Look for the worst case antenna phases

Note: the search plane here is defined as the plane that is used for the calculation of the worst case antenna phase values. This is the x-y plane that is adjacent to the platform outer plastic (at the location of the RFEM 2) and represent the worst case scenario where the user is the closest to the platform.



Figure 3 – Search Planes are the x-y planes (i.e. the transparent plane as illustrated in this picture- Left: Base plane Right: Edge plane)

Note that for xyz coordinate reference used along the report, we always consider the z-axis towards the body direction. This explains the fact that the axis convention is different between the edge and the base planes. This consideration is used to conserve a general consistency for the fields representation and calculations in the worst case determination procedure detailed below. In summary, the xy plane is the exposure plane, and z axis is the vector in propagation direction towards the body.

3.4.1 Terminology:

- Element – each one of the radiating elements that are used in the system (the antenna array has 16 radiating elements). We denote the antenna element with index **k** in this explanation.
- **N** – number of chains in the RFEM 2, **N**=16.
- Point – each point on the grid that is used for searching for the worst case position. The points are spaced 0.1mm from each other. The grid point would be denoted as **g** in this explanation.
- Complex E field vector generated by the k^{th} antenna element at point **g** :

$$\vec{E}_{k,g} = \vec{x}(\text{Re}[E_{kx,g}] + j\text{Im}[E_{kx,g}]) + \vec{y}(\text{Re}[E_{ky,g}] + j\text{Im}[E_{ky,g}]) + \vec{z}(\text{Re}[E_{kz,g}] + j\text{Im}[E_{kz,g}])$$
- Complex H field vector generated by the k^{th} antenna element at point **g** :

$$\vec{H}_{k,g} = \vec{x}(\text{Re}[H_{kx,g}] + j\text{Im}[H_{kx,g}]) + \vec{y}(\text{Re}[H_{ky,g}] + j\text{Im}[H_{ky,g}]) + \vec{z}(\text{Re}[H_{kz,g}] + j\text{Im}[H_{kz,g}])$$
- $\hat{x}, \hat{y}, \hat{z}$ – are unit direction vectors having unit magnitude and are mutually orthogonal to each other.
- Without loss of generality in this explanation RFEM 2 and search plane are in the \hat{x}, \hat{y} plane and the integrated 1cm^2 plane is perpendicular to \hat{z} direction.

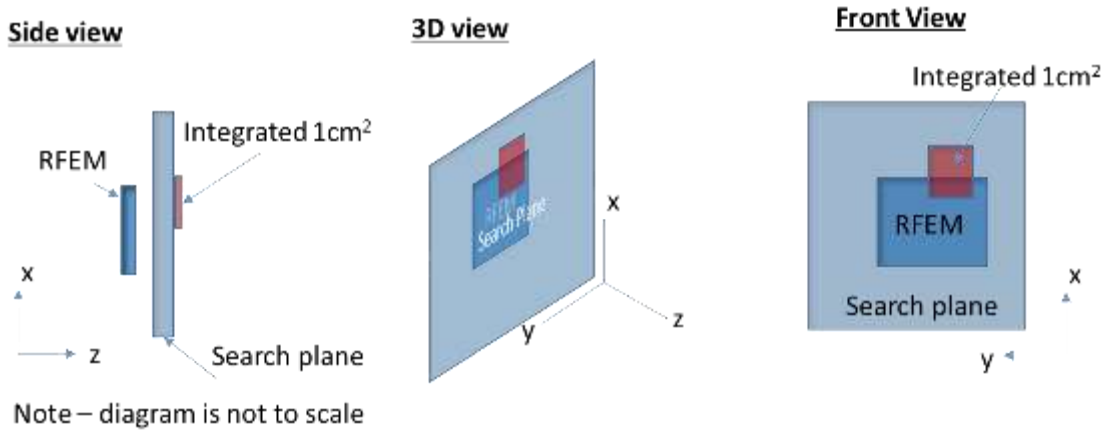


Figure 4 – Near field worst case terminology and orientation

3.4.2 Primer on field vector representation:

E and H fields generated by the k chain are:

$$\vec{E}_k = \vec{x}(\text{Re}[E_{kx}] + j\text{Im}[E_{kx}]) + \vec{y}(\text{Re}[E_{ky}] + j\text{Im}[E_{ky}]) + \vec{z}(\text{Re}[E_{kz}] + j\text{Im}[E_{kz}])$$

$$\vec{H}_k = \vec{x}(\text{Re}[H_{kx}] + j\text{Im}[H_{kx}]) + \vec{y}(\text{Re}[H_{ky}] + j\text{Im}[H_{ky}]) + \vec{z}(\text{Re}[H_{kz}] + j\text{Im}[H_{kz}])$$

E and H fields generated by all N chains are

$$\vec{E}_{\text{All}} = \vec{x} \sum_{k=1}^N (\text{Re}[E_{kx}] + j\text{Im}[E_{kx}]) + \vec{y} \sum_{k=1}^N (\text{Re}[E_{ky}] + j\text{Im}[E_{ky}]) + \vec{z} \sum_{k=1}^N (\text{Re}[E_{kz}] + j\text{Im}[E_{kz}])$$

$$\vec{H}_{\text{All}} = \vec{x} \sum_{k=1}^N (\text{Re}[H_{kx}] + j\text{Im}[H_{kx}]) + \vec{y} \sum_{k=1}^N (\text{Re}[H_{ky}] + j\text{Im}[H_{ky}]) + \vec{z} \sum_{k=1}^N (\text{Re}[H_{kz}] + j\text{Im}[H_{kz}])$$



Poynting vector generated by all N chains is

$$\begin{aligned}
 \overrightarrow{P_{\text{General,All}}} &= \frac{1}{2} \overrightarrow{E_{\text{All}}} \times \overrightarrow{H_{\text{All}}^*} \\
 &= \frac{1}{2} \langle \vec{x} \left\{ \sum_{k=1}^N (\text{Re}[E_{ky}] + j\text{Im}[E_{ky}]) \sum_{k=1}^N (\text{Re}[H_{kz}] - j\text{Im}[H_{kz}]) \right. \\
 &\quad - \sum_{k=1}^N (\text{Re}[E_{kz}] + j\text{Im}[E_{kz}]) \sum_{k=1}^N (\text{Re}[H_{ky}] - j\text{Im}[H_{ky}]) \Big\} \\
 &\quad + \vec{y} \left\{ \sum_{k=1}^N (\text{Re}[E_{kz}] + j\text{Im}[E_{kz}]) \sum_{k=1}^N (\text{Re}[H_{kx}] - j\text{Im}[H_{kx}]) \right. \\
 &\quad - \sum_{i=1}^N (\text{Re}[E_{kx}] + j\text{Im}[E_{kx}]) \sum_{k=1}^N (\text{Re}[H_{kz}] - j\text{Im}[H_{kz}]) \Big\} \\
 &\quad + \vec{z} \left\{ \sum_{k=1}^N (\text{Re}[E_{kx}] + j\text{Im}[E_{kx}]) \sum_{k=1}^N (\text{Re}[H_{ky}] - j\text{Im}[H_{ky}]) \right. \\
 &\quad - \sum_{k=1}^N (\text{Re}[E_{ky}] + j\text{Im}[E_{ky}]) \sum_{k=1}^N (\text{Re}[H_{kx}] - j\text{Im}[H_{kx}]) \Big\} \rangle
 \end{aligned}$$

Power flow is

$$\begin{aligned}
 \text{Re}[\overrightarrow{P_{\text{General,All}}}] &= \frac{1}{2} \langle \vec{x} \left\{ \sum_{k=1}^N \text{Re}[E_{ky}] \sum_{k=1}^N \text{Re}[H_{kz}] + \sum_{k=1}^N \text{Im}[E_{ky}] \sum_{k=1}^N \text{Im}[H_{kz}] - \sum_{k=1}^N \text{Re}[E_{kz}] \sum_{k=1}^N \text{Re}[H_{ky}] \right. \\
 &\quad - \sum_{k=1}^N \text{Im}[E_{kz}] \sum_{k=1}^N \text{Im}[H_{ky}] \Big\} \\
 &\quad + \vec{y} \left\{ \sum_{k=1}^N \text{Re}[E_{kz}] \sum_{k=1}^N \text{Re}[H_{kx}] + \sum_{k=1}^N \text{Im}[E_{kz}] \sum_{k=1}^N \text{Im}[H_{kx}] - \sum_{k=1}^N \text{Re}[E_{kx}] \sum_{k=1}^N \text{Re}[H_{kz}] \right. \\
 &\quad - \sum_{k=1}^N \text{Im}[E_{kx}] \sum_{k=1}^N \text{Im}[H_{kz}] \Big\} \\
 &\quad + \vec{z} \left\{ \sum_{k=1}^N \text{Re}[E_{kx}] \sum_{k=1}^N \text{Re}[H_{ky}] + \sum_{k=1}^N \text{Im}[E_{kx}] \sum_{k=1}^N \text{Im}[H_{ky}] - \sum_{k=1}^N \text{Re}[E_{ky}] \sum_{k=1}^N \text{Re}[H_{kx}] \right. \\
 &\quad - \sum_{k=1}^N \text{Im}[E_{ky}] \sum_{k=1}^N \text{Im}[H_{kx}] \Big\} \rangle
 \end{aligned}$$

Power flow to Z is

$$\begin{aligned}
 \vec{z} \cdot \text{Re}[\overrightarrow{P_{\text{General,All}}}] &= \frac{1}{2} \langle \left\{ \sum_{k=1}^N \text{Re}[E_{kx}] \sum_{k=1}^N \text{Re}[H_{ky}] + \sum_{k=1}^N \text{Im}[E_{kx}] \sum_{k=1}^N \text{Im}[H_{ky}] - \sum_{k=1}^N \text{Re}[E_{ky}] \sum_{k=1}^N \text{Re}[H_{kx}] \right. \\
 &\quad - \sum_{k=1}^N \text{Im}[E_{ky}] \sum_{k=1}^N \text{Im}[H_{kx}] \Big\} \rangle
 \end{aligned}$$

3.4.3 Domain search for worst case direction

The two domain search is completed as follows:

- First find a direction (location) for the worst case 1cm^2 square averaging area using upper bound methods.

The basic concept behind the upper bound method is to assume that there could be an "ideal beam forming" mechanism that could align the phases of all the elements for both E and H field (obviously in real life this cannot happen – this is the reason that this is an upper bound method). When this ideal mechanism is used then all the complex phasors are aligned to the same phase, hence the phasor absolute value can be used instead of the phasor \rightarrow the E (and H) field for any direction is the sum of the magnitude of the fields (look at item 3 below for more formal description).

This method provides the worst case position independent of the antenna phases \rightarrow it allows finding the worst case location with this "ideal beam forming" mechanism. Item 3 below translate the above verbal description to more formal mathematical wording.

- After the worst case direction is found using the upper bound method, the antenna phases are aligned to this direction. The antenna phases are aligned to maximize the power across the 1cm^2 averaging area that was found using the upper bound method. The method that is used to find the required antenna phases is: first order the antenna according to the power contribution on the found 1cm^2 from the highest to the lowest. Then start by activating the antenna that contribute the most and set its phase to 0, then activate the 2nd antenna and search over the phases for the 2nd antenna. Choose the phase that maximize the power of the two antenna elements. For finding the phase for the third antenna fix antenna 1 phase to zero and the 2nd antenna to the value that was found before – now search for the phases for the third antenna phases that maximize the power. Continue with the same process till the 16th element.
- Calculate the power density with the antenna phases that were found in the previous item (item B).

The above process can be written as the following algorithm:

- A grid is defined with 0.1mm spacing.
- At each point in the grid, the complex E & H fields are calculated using each one of the 16 radiating elements separately. Each one of the calculated E & H fields are 3D complex vectors, so the simulation output from this stage is 16 3-D complex E field strength vectors and 16 3D complex H field strength vectors. The vectors are defined as:

$$\overrightarrow{E_{k,g}} = \vec{x}(\text{Re}[E_{kx,g}] + j\text{Im}[E_{kx,g}]) + \vec{y}(\text{Re}[E_{ky,g}] + j\text{Im}[E_{ky,g}]) + \vec{z}(\text{Re}[E_{kz,g}] + j\text{Im}[E_{kz,g}])$$
 and

$$\overrightarrow{H_{k,g}} = \vec{x}(\text{Re}[H_{kx,g}] + j\text{Im}[H_{kx,g}]) + \vec{y}(\text{Re}[H_{ky,g}] + j\text{Im}[H_{ky,g}]) + \vec{z}(\text{Re}[H_{kz,g}] + j\text{Im}[H_{kz,g}])$$
- Upper bound assumption is used to derive the E & H field on each one of the grid point, the following items describe the upper bound method that is used:
 - The calculation is made separately for E field and H field.
 - For E field the following calculation is made independently for each one of the grid point:

$$\begin{aligned} \overrightarrow{E_{UB,g}} &= \vec{x} \sum_{k=1}^N \sqrt{\text{Re}[E_{kx,g}]^2 + \text{Im}[E_{kx,g}]^2} + \vec{y} \sum_{k=1}^N \sqrt{\text{Re}[E_{ky,g}]^2 + \text{Im}[E_{ky,g}]^2} \\ &\quad + \vec{z} \sum_{k=1}^N \sqrt{\text{Re}[E_{kz,g}]^2 + \text{Im}[E_{kz,g}]^2} = \vec{x} \sum_{k=1}^N |E_{kx}| + \vec{y} \sum_{k=1}^N |E_{ky}| + \vec{z} \sum_{k=1}^N |E_{kz}| \end{aligned}$$

The magnitude of the complex E vector is summed over the antenna elements. The summation is being done for each one of the grid point and for each one for each direction independently.



- c. The output of the previous item is 3D real vector of the E field on each one of the simulated grid points in each direction. The physical implementation is that an ideal beam forming was done for the E field for each one of the points.
- d. Same process as described in item b is being done for the H field.

$$\begin{aligned} \overrightarrow{H_{UB,g}} &= \vec{x} \sum_{k=1}^N \sqrt{\operatorname{Re}[H_{kx,g}]^2 + \operatorname{Im}[H_{kx,g}]^2} + \vec{y} \sum_{k=1}^N \sqrt{\operatorname{Re}[H_{ky,g}]^2 + \operatorname{Im}[H_{ky,g}]^2} \\ &+ \vec{z} \sum_{k=1}^N \sqrt{\operatorname{Re}[H_{kz,g}]^2 + \operatorname{Im}[H_{kz,g}]^2} = \vec{x} \sum_{k=1}^N |H_{kx,g}| + \vec{y} \sum_{k=1}^N |H_{ky,g}| + \vec{z} \sum_{k=1}^N |H_{kz,g}| \end{aligned}$$

- e. In each point in the grid the poynting vector is calculated by vector multiplication of E & H field which are added-up in items b & d. As explained before, without loss of generality we assume that the search plane is X/Y plane and the energy propagate to Z dimension, this translates to:

$$\begin{aligned} P_{g,z} &= \frac{1}{2} \operatorname{Re}\{\hat{z} \cdot (\vec{E} \times \vec{H}^*)\} = \frac{1}{2} \operatorname{Re}\{\hat{z} \cdot ((\dots) \hat{x} + (\dots) \hat{y} + (E_x H_y^* - E_y H_x^*) \hat{z})\} = \\ &= \frac{1}{2} \operatorname{Re}\{E_x H_y^* - E_y H_x^*\} \leq \frac{1}{2} |E_x H_y^* - E_y H_x^*| \leq \\ &\leq \frac{1}{2} |E_x H_y^*| + \frac{1}{2} |E_y H_x^*| = \frac{1}{2} \{|E_x| \cdot |H_y| + |E_y| \cdot |H_x|\} = \\ PUpperBound_{z,g} &= \frac{1}{2} \langle \sum_{i=1}^N |E_{ix}| \sum_{i=1}^N |H_{iy}| + \sum_{i=1}^N |E_{iy}| \sum_{i=1}^N |H_{ix}| \rangle \end{aligned}$$

The final value $(\frac{1}{2} \langle \sum_{i=1}^N |E_{ix}| \sum_{i=1}^N |H_{iy}| + \sum_{i=1}^N |E_{iy}| \sum_{i=1}^N |H_{ix}| \rangle)$ obtained in each grid point represents an upper bound value i.e. this value is always greater than or equal to the real pointing vector magnitude $(\frac{1}{2} \operatorname{Re}\{\hat{z} \cdot (\vec{E} \times \vec{H}^*)\})$.

- 4. The above calculated poynting vectors are used to estimate the power across 1cm^2 area. Note that in this example the relevant direction for the pointing vector is \hat{z} direction

$$P1cm2 = \iint_{1\text{cm}^2} \overrightarrow{PUpperBound_{g,x,y,z}} \cdot \hat{z}$$

- 5. The 1cm^2 area with the highest power value is used as the worst case the direction. The antenna phases are aligned to maximize the energy in this 1cm^2 area as explained below:

- a. Turn on each element one-by-one to find order of power intensity in the 1cm^2 window.
(Find the order of contribution)
- b. Sort in the power order from the highest to the lowest #0 to #15.
- c. Turn on #0 with phase $P0=0$. (reference)
- d. Turn on #1 and change phase to maximize the power and find the phase $P1$.
- e. Keep $P0$ and $P1$, turn on #2 and do same.
- f. Repeat for the rest of the antennas.

- 6. Using the antenna phases that were calculated in step 6 the power density is calculated along the base plane.

3.5 3D Models Used in the Simulation

3.5.1 Worst case operating conditions of the platform

The platform Lenovo TP00076B is a special platform with the ability to rotate the screen by 360°. This ability allows the platform to work in various operation modes, as can be seen in the Figure 5.



Figure 5 - Platform operating modes

The worst case condition regarding the radiated near field was found for Tablet operating mode. When Tablet operating mode is set, the lid is rotated by 360 where the screen is folded over on top of the keyboard as shown on the Figure 6.



Figure 6 - Platform worst case operating mode



3.5.2 RFEM 2 housing inside Intel 18260NGW module

3D Intel 18260NGW module CAD files are used in the EM simulation to allow correct exposure level simulation.

Please refer to the following picture only as a reference to visualize RFEM 2 placement inside the Lenovo Model TP00076B platform.



Figure 7 – Active antenna inside the platform

3.5.3 Closest distance to the body of an end user

The highest RF exposure was found when the platform is configured in tablet mode, the screen is flipped to the backside of the keyboard. The minimum distance between the active antennas to the skin of an end user is when the person holding the unit and touching the plastic. For this configuration, 2 planes have been simulated, one on the base as shown on the Figure 8 and the second one on as shown on the Figure 9. The minimum distance between a hand or body to the active antenna is 13.9 mm for the simulated plane on the base and 6.0 mm for the simulated plane on edge.

In this section are presented the simulation results of the platform configured in tablet mode. The area simulated is located on the base, as shown in blue on the Figure 28.



Figure 8 – Simulated area on the base

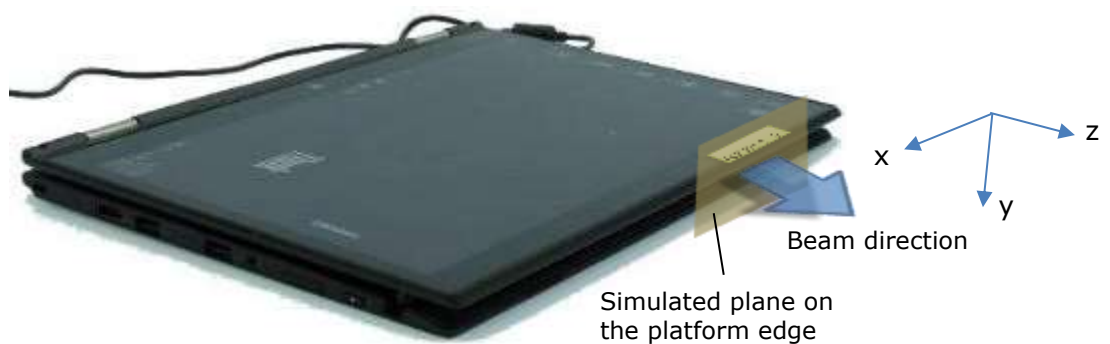


Figure 9 – Simulated area on the edge

3.5.4 Metals in proximity of the RFEM 2

All the metals that are in the RFEM 2 region (10mm on each side) were included in the simulation.



3.6 Antenna feed

The following gives a general description of the numerical simulations; other details of the simulation geometry are included in the confidential Operational Description exhibit. The EM simulation uses an accurate 3D model of the RFEM 2 antenna. The model includes the antenna elements as well as their feeding lines. Both PCBs (antenna PCB and Si PCB) are simulated. The simulation starts at the silicon bumps (the metal bump that is connected to the Silicon and soldered to the board).

In the simulation, we excite the antennas at the silicon output port (the antenna structure includes the vias, traces and actual antenna element). Please note that the output ports are used as the interface from the Si to the antenna. The Si output are localized in the Si side, while looking from the PCB + antenna direction we can find the antenna feed points. The RFEM 2 layers are fully simulated, including all parts of the PCB and antennas boards: conducted traces, feeds, antenna elements and dielectrics. The mesh resolution is automatically defined by the simulation tool to assure better than 2% simulation convergence precision.

Signals with equal level are applied for the 16 antenna chains. The simulation uses a fixed power feed per element, such that the aggregated conducted output power at the antenna feed points is 6 dBm. In other words each one of the 16 elements is fed by -6dBm such that the total conductive equivalent power is 16 times -6dBm, so +6dBm. In addition, the simulation is conducted using 100% TX duty cycle.

The total power (same per element) is used to build the pattern of radiated power through beam forming. For building the beamforming pattern the same power is used per element, while phase is changed per element, please look at chapter 2.2 for more information about the beamforming. Phases are derived for each excitation separately to simulate the worst case condition. Chapter 3.4 explains how the phases are derived to find worst case condition.

4 Simulation Results

As described in the section 3.5.3 two planes have been simulated, the power density of both planes results are presented in this section.

The power density has been simulated over 3 channels, for each channel we'll present the results detail according to the methodology explained in section 3.4:

- Simulation results of the single-point power density for each single-point across the Mesh ($P_{UpperBound_{z,g}}$) and the worst case coordinate (Figure 11 to Figure 13 for edge plane and Figure 25 to Figure 27 for base plane). Please note that this value is single-point power density and not integrated power density over 1cm^2 (even though 1mW/cm^2 scale is used, this value represents an upper bound power density for each single-point of the mesh which is much smaller area than 1cm^2).
- The results of the single-point power density in z direction using the antenna phases corresponding to the worst case coordinate found above (Figure 15 to Figure 17 for edge plane and Figure 29 to Figure 31 for base plane). In this section correction factors are presented, these factors are the ratios between the single-point power density using the z component of Poynting vector and the single-point power density using the three components of Poynting vector. These factors are presented in Table 3 of section 4.1.2 and Table 7 of section 4.2.2.
- One dimensional cut of the mesh single-point power density – showing 1 dimensional cut of the mesh power density (Figure 18 to Figure 20 for edge plane and Figure 36 to Figure 38 for base plane). In the XY plane, the X cut is done with the Y in the maximum value, similarly Y cut is done with the X in the maximum value. These results show the results using the z component of the Poynting vector.
- Integrated power density over 1cm^2 – these figures present the integrated power density across 1cm^2 using the z component of Poynting vector (Figure 21 to Figure 23 for edge plane and Figure 39 to Figure 41 for base plane). Each point in the figure represents integration over 1cm^2 , where the point location is the location of the center of the square
- The worst case power-density in z direction integrated over 1cm^2 using the worst case antenna phases computed by the simulation (Figure 25 to Figure 27 for edge plane and Figure 42 to Figure 44 for base plane) and the final value at zero distance obtained by the application of the scaling factors between normal and global Poynting vector components. (Table 5 for edge plane and Table 9 for base plane).

4.1 Results on the Edge area

In this section are presented the simulation results of the platform configured in tablet mode. The area simulated is located on the edge, as shown in blue on the Figure 10. Z direction (Beam direction) is the direction towards the body.



Figure 10 – Edge plane illustration

4.1.1 Upper bound simulation results for edge plane exposure

The Figure 11, Figure 12 and Figure 13 present upper bound Z single-point power density as described in section 3.4.

In each one of the figures the worst case 1cm^2 is plotted in the figure, and the co-ordinate of the center of the 1cm^2 is given (0,0 for the co-ordination system is lower left corner of the plots). Please note that since the worse-case conditions are searched over a plane for near field, then the azimuth and the elevation are not relevant. The worst case position is calculated using all the power density single-point issued from the upper bound simulation results. The upper bound worst case Z power density distributions for three channels are are shown in Figure 11, Figure 12 and Figure 13. We leverage the phase conditions (summarized in Table 2) for each antenna element that resulted in these worst case conditions to evaluate final integrated power density. The mathematical basis for using these as the worst case phase conditions to evaluate the final integrated power density is provided in Section 3.4.3.

The plane dimensions of the Z single-point power density results is 49.5 mm x 23.3 mm (Figure 11, Figure 12 and Figure 13).

The footprint of the platforms components in the edge plane for single-point power density representation is showed in Figure 14.

Worst case coordinate on channel 1 are X = 26 mm, Y = 15.2mm.

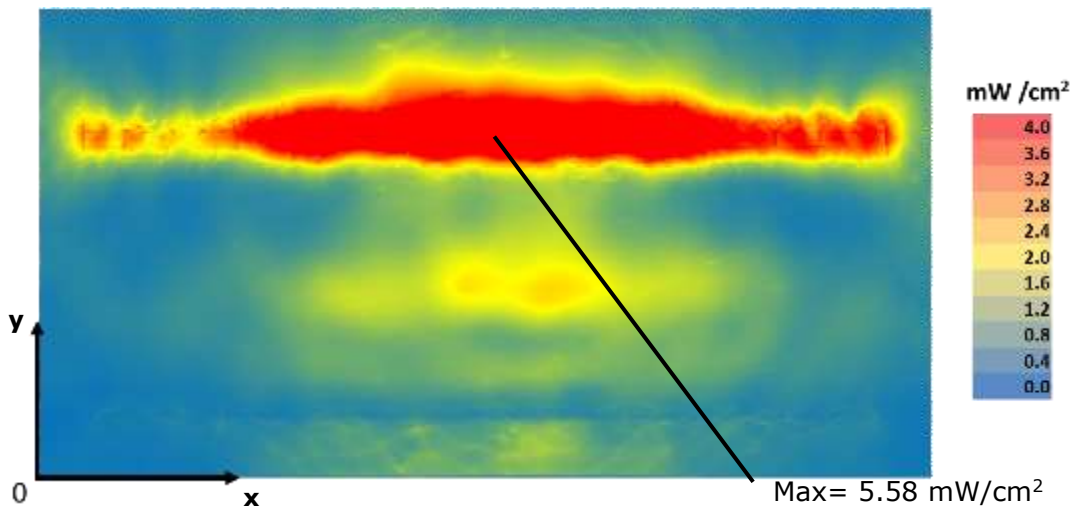


Figure 11 – Channel 1 upper bound, Single-point Power Density mesh on platform edge

Worst case coordinate on channel 2 are X= 26 mm, Y = 14.5mm.

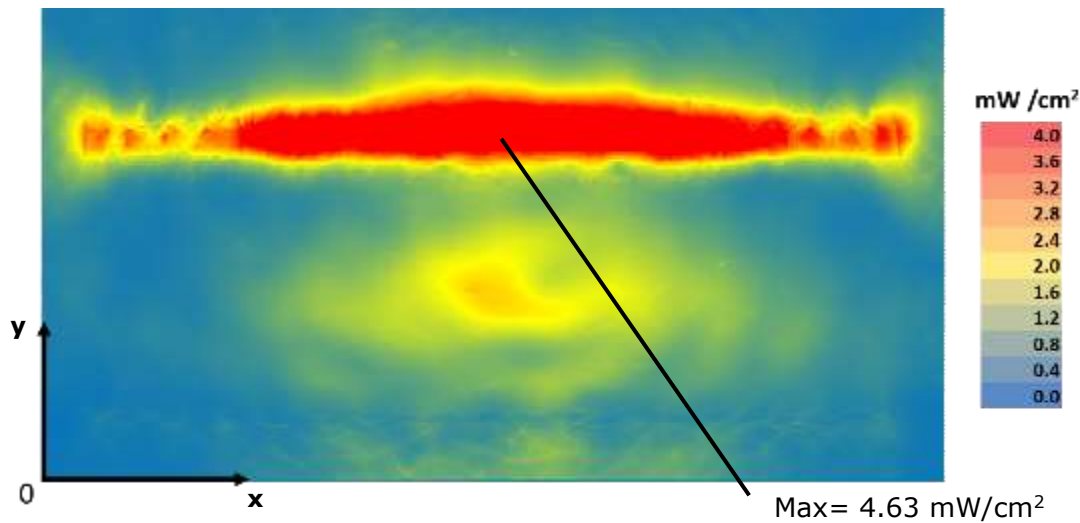


Figure 12 – Channel 2 upper bound, Single-point Power Density mesh on platform edge

Worst case coordinate on channel 3 are X = 26.2 mm, Y = 14.8 mm.

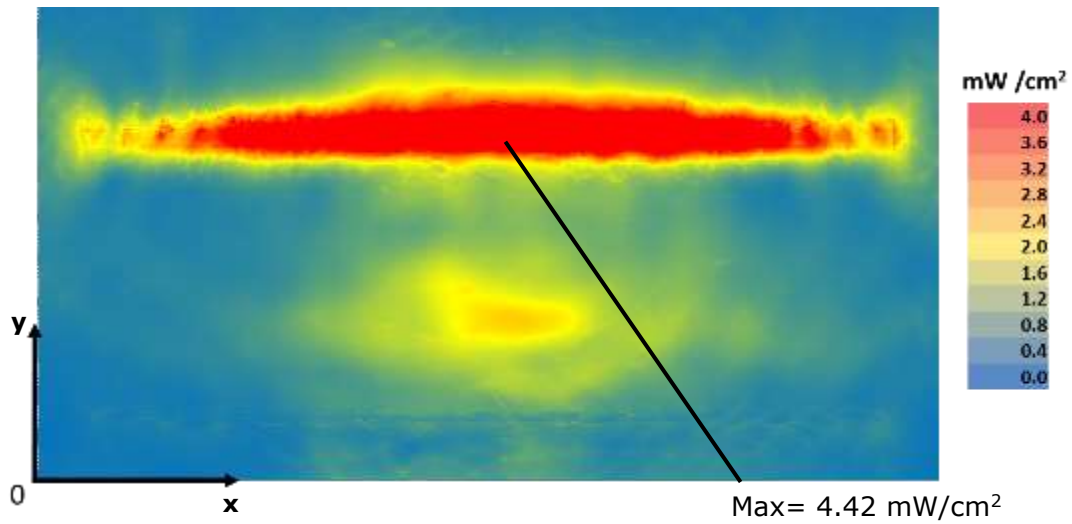


Figure 13 – Channel 3 upper bound, Single-point Power Density mesh on platform edge

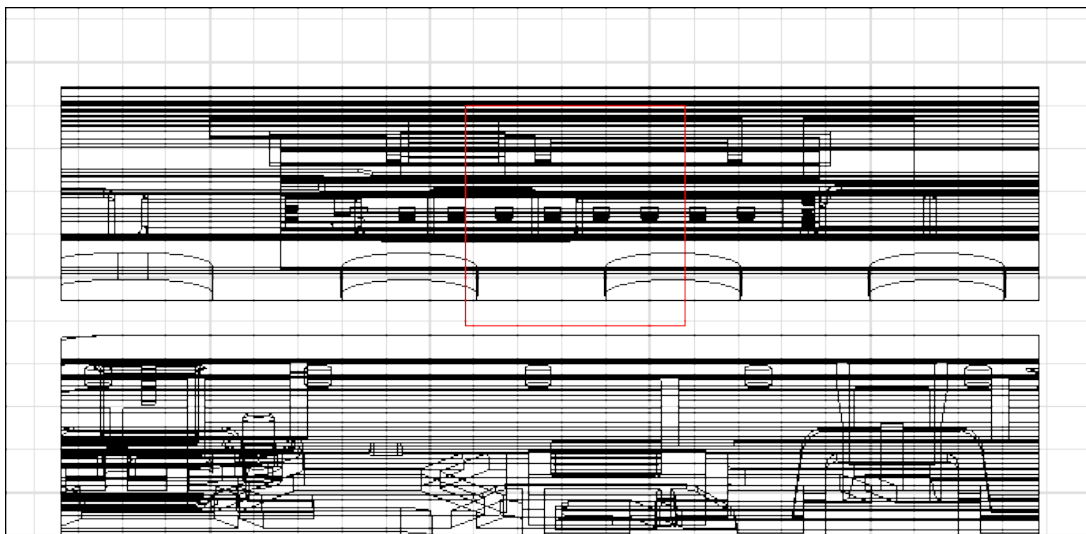


Figure 14 – Footprint of single-point power density plane representation in edge plane

4.1.2 Single-point power density values with worst-case antenna phases for edge plane exposure

The Table 2 shows the phase for each antenna elements per channel for the worst case found as described in the chapter 3.4. The phases search algorithm is detailed in point 5 of the section 3.4.3.

| Antenna index | Phases [Degrees] | | |
|---------------|------------------|-----------|-----------|
| | Channel 1 | Channel 2 | Channel 3 |
| 0 | 0 | 90 | 45 |
| 1 | 90 | 135 | 90 |
| 2 | 180 | 225 | 180 |
| 3 | 0 | 0 | 0 |
| 4 | 0 | 0 | 45 |
| 5 | 90 | 90 | 90 |
| 6 | 180 | 180 | 180 |
| 7 | 0 | 0 | 0 |
| 8 | 0 | 0 | 45 |
| 9 | 45 | 90 | 135 |
| 10 | 135 | 180 | 225 |
| 11 | 315 | 315 | 0 |
| 12 | 315 | 315 | 45 |
| 13 | 45 | 45 | 135 |
| 14 | 135 | 180 | 225 |
| 15 | 315 | 315 | 45 |

Table 2 – Phases configurations for the worst case

The amplitude on each antenna is -6dBm as explained in chapter 3.6.

The Figure 15, Figure 16 and Figure 17 present power density in the body direction using worst case antenna phases presented in the Table 2. The simulated power density area has a size of is 49.5 mm x 23.3 mm, this area corresponds to the blue delimitation.

Table 3 presents the ratios (linear and logarithmic) at the highest single-point value for the Z trajectory on the edge area between the power density worst case value along the body direction (S_z) and the power density worst case value along the propagation direction (S_{tot}) for all channels and taking into account all components. This table confirms that the power density component along Z is the major contributor in the total power density. Also the ratios are used for results scaling in Table 6 of section 4.1.5 and in the compliance summary discussion in section 6 .

| EDGE AREA | Channel 1 | Channel 2 | Channel 3 |
|--|-----------|-----------|-----------|
| Mag S_{tot} (maximum poynting single-point value with all components) [mW/cm ²] | 4.181 | 4.243 | 2.553 |
| S_z (trajectory of the above on Z direction) [mW/cm ²] | 2.495 | 2.217 | 2.292 |
| Ratio (S_z / S_{tot}) [linear] | 0.597 | 0.522 | 0.898 |
| Ratio $10\log(S_z / S_{tot})$ [dB] | -2.24 | -2.82 | -0.46 |

Table 3 – Ratios between Z-power density and total power density on edge area

Worst case coordinate on channel 1 are X = 25.9 mm, Y = 14.1 mm.

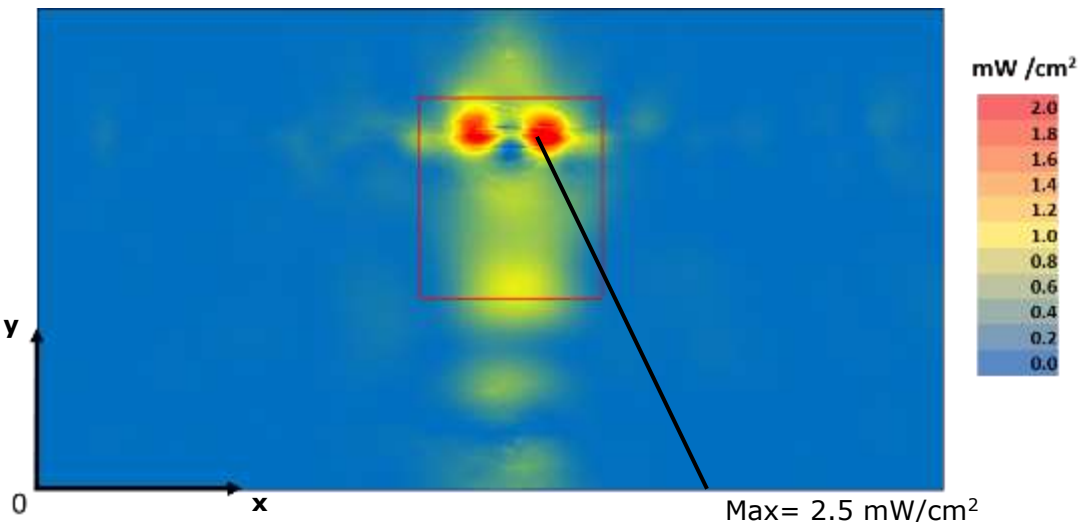


Figure 15 – Channel 1 single-point power density mesh on platform edge

Worst case coordinate on channel 2 are X = 25.3 mm, Y = 14.1 mm.

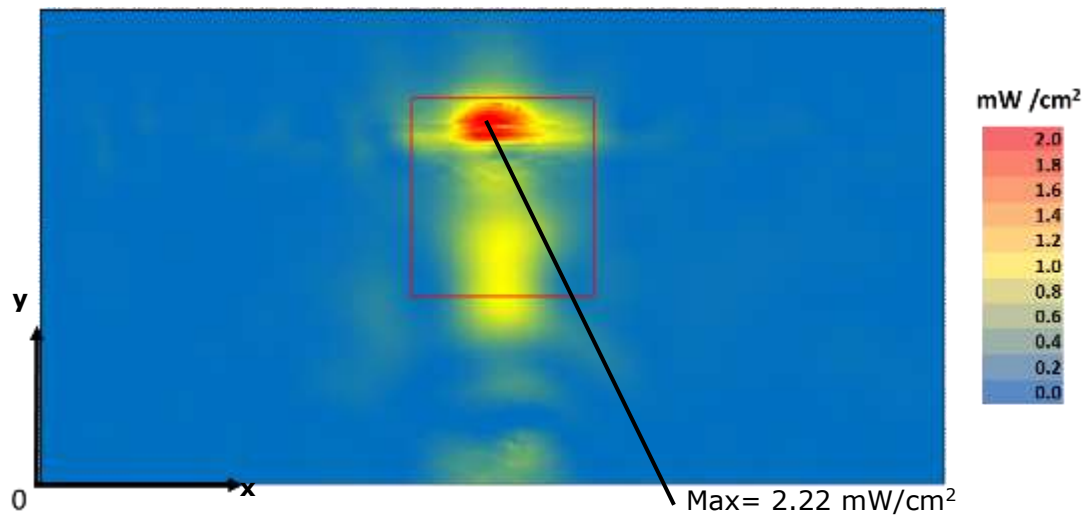


Figure 16 – Channel 2 single-point power density mesh on platform edge

Worst case coordinate on channel 3 are X = 26 mm, Y = 16.1 mm.

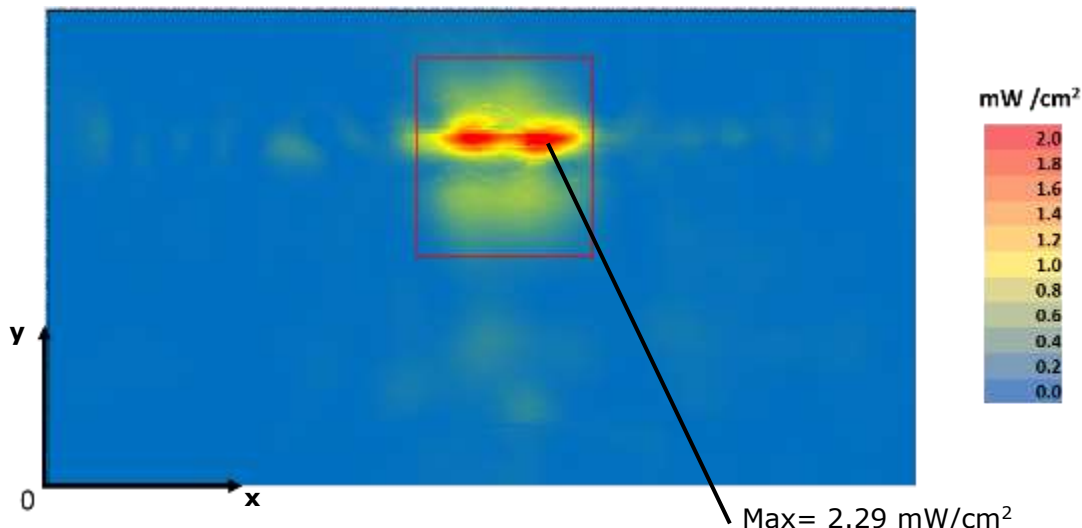


Figure 17 – Channel 3 single-point power density mesh on platform edge

The highest value shown in these figures is a point and not yet integrated over the 1cm^2 . The final power density value is given in section 4.1.5.

4.1.3 One dimensional cut of the mesh single-point power density for edge plane exposure

In Figure 18 – Figure 20 below, we present a subset of the simulation results from the Z-component of single-point power density values with worst antenna phases (Chapter 4.1.2).

The subset is a 1 dimensional cut in the X axis and Y axis that shows the behavior of the near field power density at zero distance.

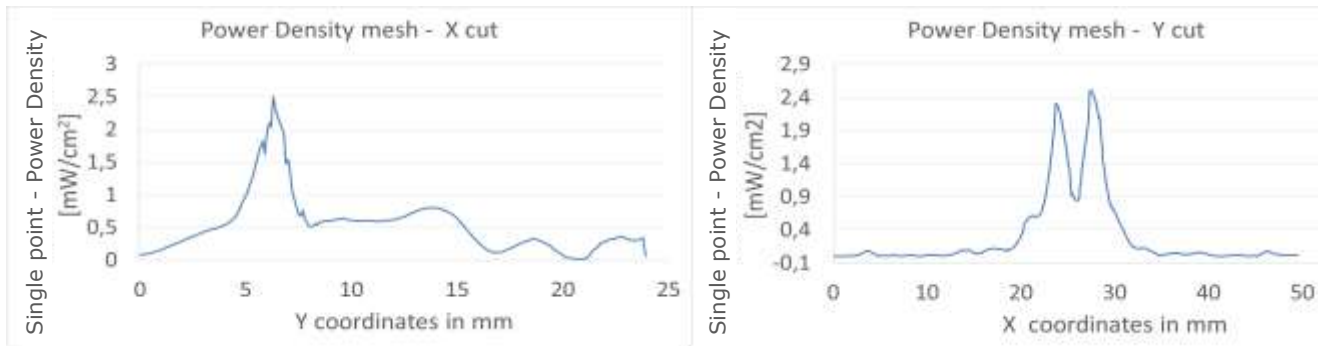


Figure 18 – One dimensional plots of the power density on Channel 1

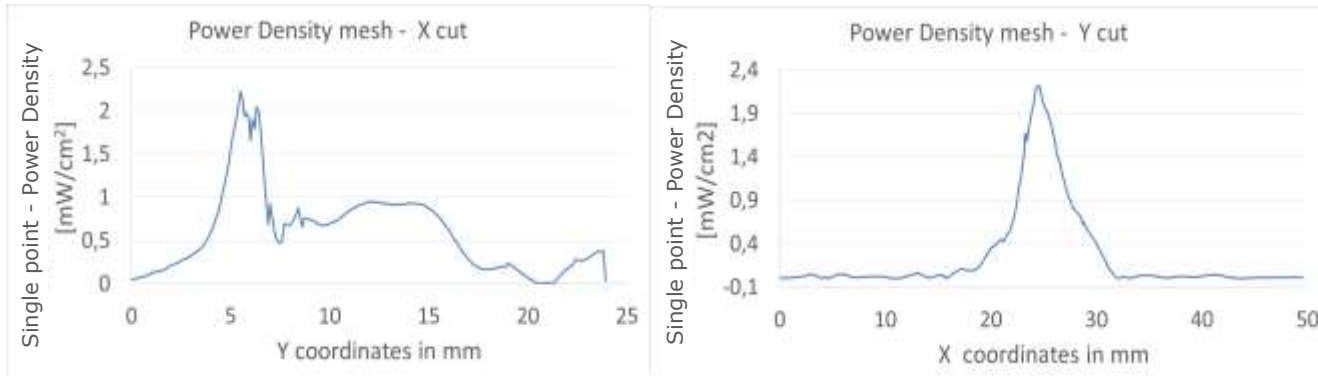


Figure 19 – One dimensional plots of the power density on Channel 2



Figure 20 – One dimensional plots of the power density on Channel 3

4.1.4 Integrated power density over 1 cm² for edge plane exposure

The Figure 21 - Figure 23 below present the Z-integrated power over 1cm² at 100% duty cycle for the worst case scenario as explained in section 3.4.3. The plane dimensions of these results is 39.5 mm x 13.3 mm.

The 1cm² square location correspondent to the maximum of integrated power density value for each channel is plotted in red in figures below (Figure 21 - Figure 23). The maximum average values are mentioned in the second row of Table 4. The worst case coordinates are the center of the squares.

The footprint of the platforms components in the edge plane for integrated power density representation is showed in Figure 24.

Worst case coordinate on channel 1 are X= 20.9 mm, Y = 9.1 mm.

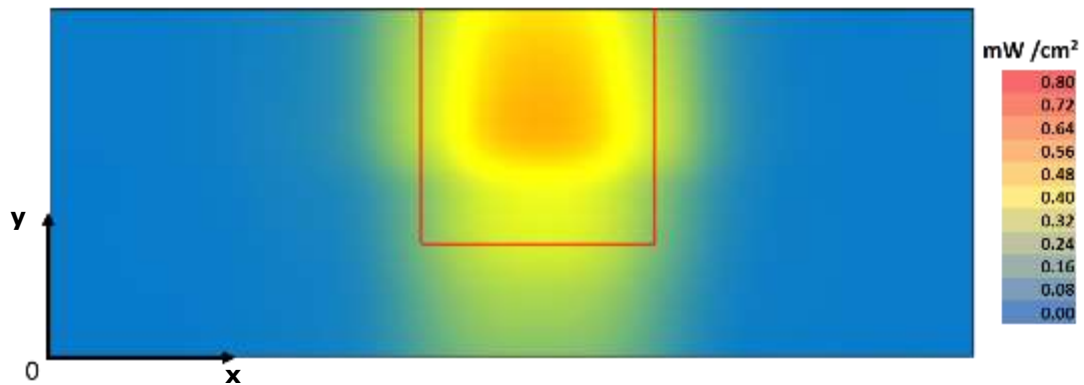


Figure 21 – Channel 1 worst case - Integrated power over 1cm² an platform edge

Worst case coordinate on channel 2 are X= 20.3 mm, Y = 9.1 mm

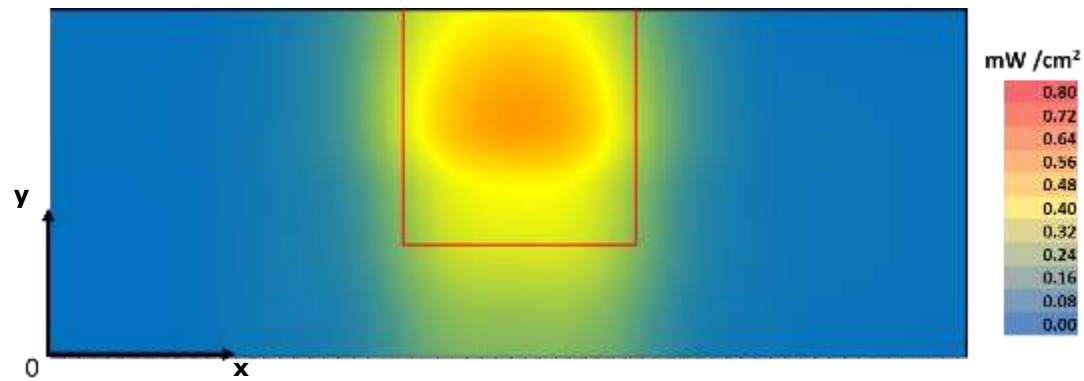


Figure 22 – Channel 2 worst case - Integrated power over 1cm² an platform edge

Worst case coordinate on channel 3 are X = 21 mm, Y = 11.1 mm

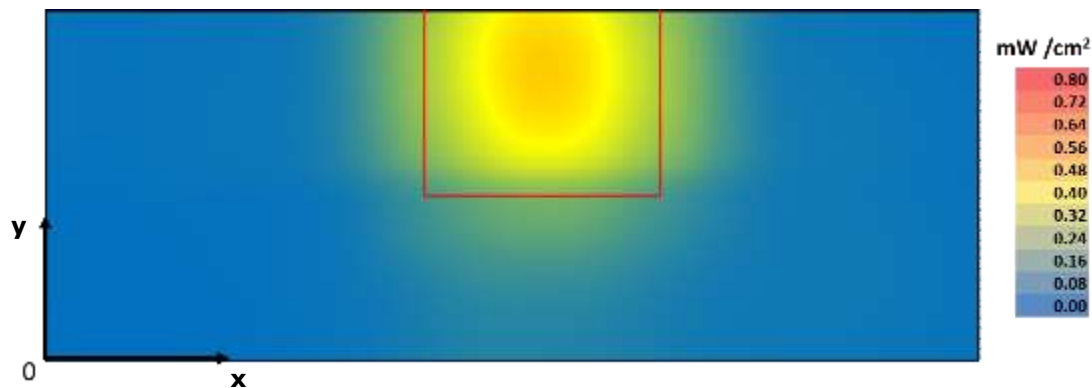


Figure 23 – Channel 3 worst case - Integrated power over 1cm² an platform edge



Figure 24 – Footprint of integrated power density plane representation in edge plane

4.1.5 Power density for edge plane exposure

The Figure 25, Figure 26 and Figure 27 show the worst case power-density integrated over 1cm² versus the distance. As described in section 3.4.3 and section 3.5.2 the worst case was computed by the simulation using the worst case antenna phases and the worst platform configuration (Tablet mode). The 0mm reference correspond to the platform boundary, the active antenna located inside the platform is at 8.46 mm from this distance.

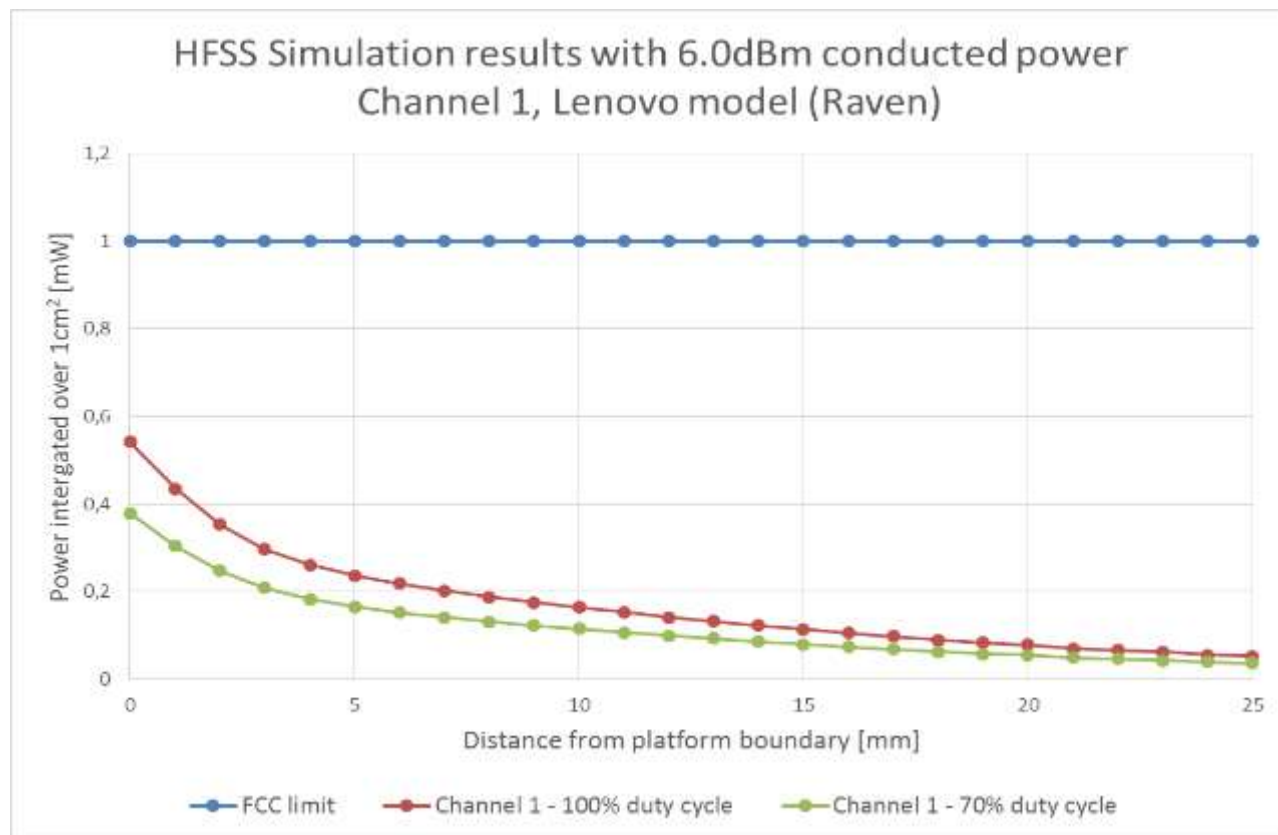


Figure 25 – HFSS Simulation results in Ch1 (Edge plane)

HFSS Simulation results with 6.0dBm conducted power
Channel 2, Lenovo model (Raven)

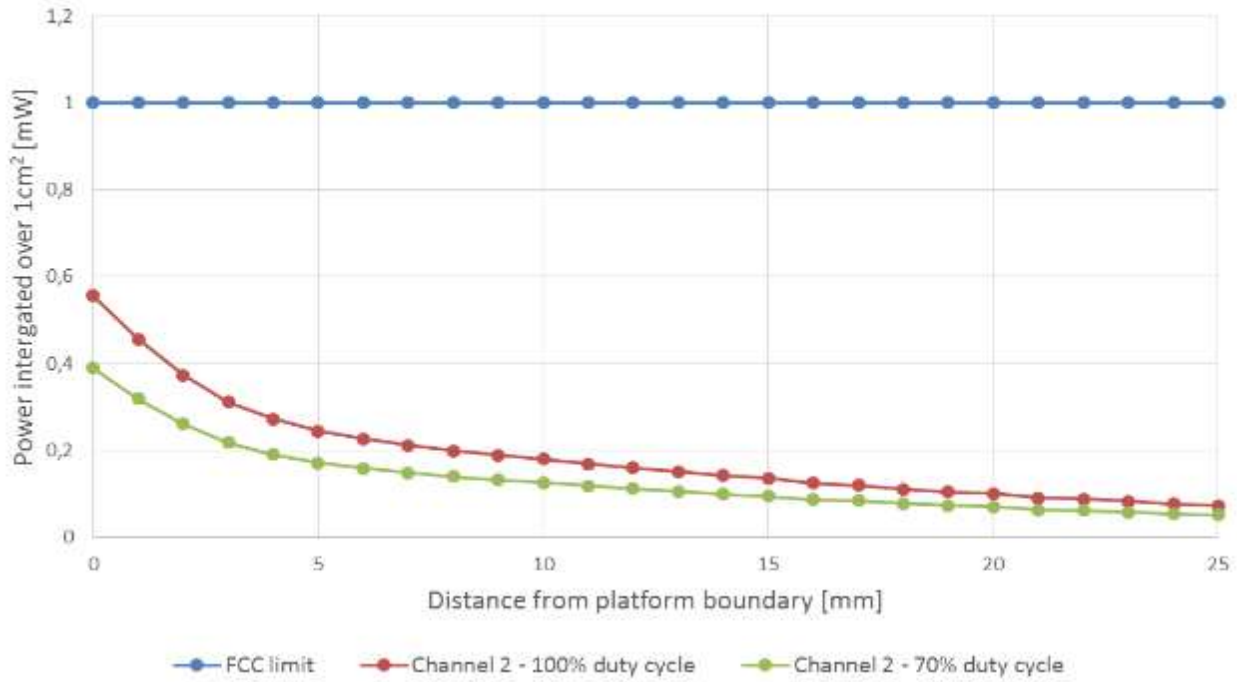


Figure 26 – HFSS Simulation results in Ch2 (Edge plane)

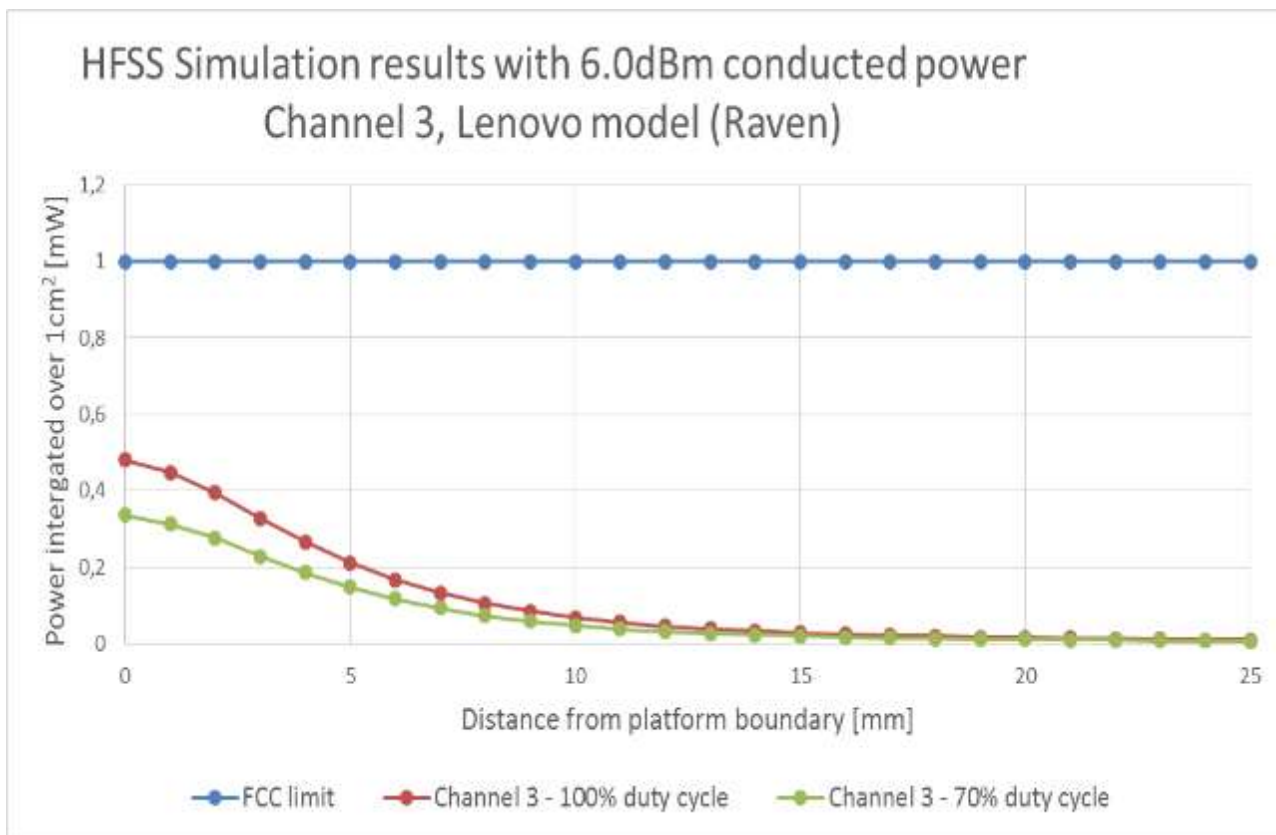


Figure 27 – HFSS Simulation results in Ch3 (Edge plane)

The Table 4 show the simulated worst case power dentisty at the edge plane area for each channels.

| Edge plane Highest power density | Channel 1 [mW/cm ²] | Channel 2 [mW/cm ²] | Channel 3 [mW/cm ²] |
|-------------------------------------|------------------------------------|------------------------------------|------------------------------------|
| 70% duty cycle | 0.379 | 0.390 | 0.336 |
| 100% duty cycle | 0.541 | 0.557 | 0.480 |

Table 4 – Worst case power density - Edge plane



Notes for Table 4:

1. The worst case channel is channel 2.
2. The Maximum power density (spatially integrated over worst 1cm²) in channel 2 (worst case) is achieved at 0mm distance from the platform boundary and equals to 0.557 mW/cm² over 100% duty cycle.
3. As explained in section 2.3, the Intel 18260NGW module is limited to Transmit at a duty cycle of 70% over 10seconds. Therefore the maximum spatially integrated and time averaged power density over 1cm² is 0.557 x 0.7 = 0.390 mW/cm².
4. Taking into account the ratios presented in Table 3 between the Z-component and the total power density, the integrated power densities values at zero distances become:

| | Channel 1 | Channel 2 | Channel 3 |
|---|------------------|------------------|------------------|
| Integrated Power density in Z-direction (P_z) [mW/cm²] | 0.379 | 0.390 | 0.336 |
| Corresponding Ratio (R) | 0.597 | 0.522 | 0.898 |
| Global Integrated Power density ($P_{tot}=P_z/R$) [mW/cm²] | 0.637 | 0.747 | 0.379 |

Table 5 – Edge plane integrated power density at zero distance

Therefore, the worst case channel remains channel 2 and the maximum spatially integrated and time averaged total power density over 1cm² is 0.390 / 0.522 = 0.747 mW/cm².

4.2 Results on the Base area.

In this section are presented the simulation results of the platform configured in tablet mode. The area simulated is located on the base, as shown in grey on the Figure 28. Z direction (Beam direction) is the direction towards the body.

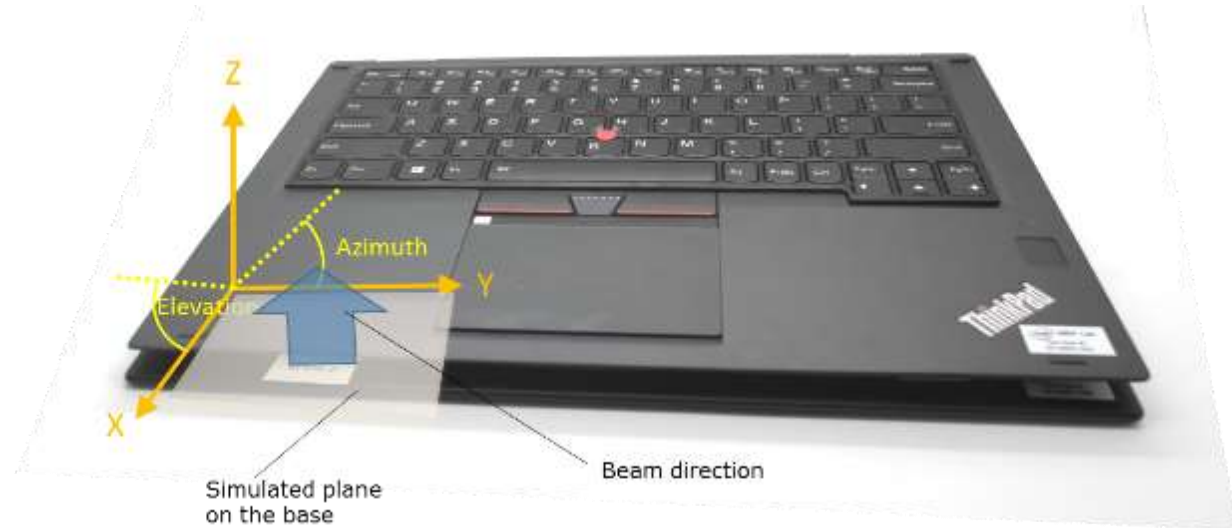


Figure 28 –Base plane illustration

4.2.1 Upper bound simulation results for base plane exposure

The figures below present upper bound Z single-point power density (as described in section 3.4). In each figure the single-point power (in mW/cm^2) is shown as well as the place of this maximum value.

Please note that since the worse-case conditions are searched over a plane for near field, then the azimuth and the elevation are not relevant. The worst case position is calculated using all the power density single-point issued from the upper bound simulation results. The upper bound worst case Z power density distributions for three channels are shown in Figure 29, Figure 30 and Figure 31. We leverage the phase conditions (summarized in Table 6) for each antenna element that resulted in these worst case conditions to evaluate final integrated power density. The mathematical basis for using these as the worst case phase conditions to evaluate the final integrated power density is provided in Section 3.4.3.

The plane dimensions of the single-point power density results is 49.5 mm x 32.4 mm (Figure 29, Figure 30 and Figure 31).

Please note that in the top left of each figure there is an area with ~ 0 energy, this is explained by the fact that there is metal in this place in the platform and is an expected result.

The footprint of the platforms components in the base plane for single-point power density representation is showed in Figure 32

Worst case coordinate on channel 1 are X= 24.3 mm, Y = 15.5 mm.

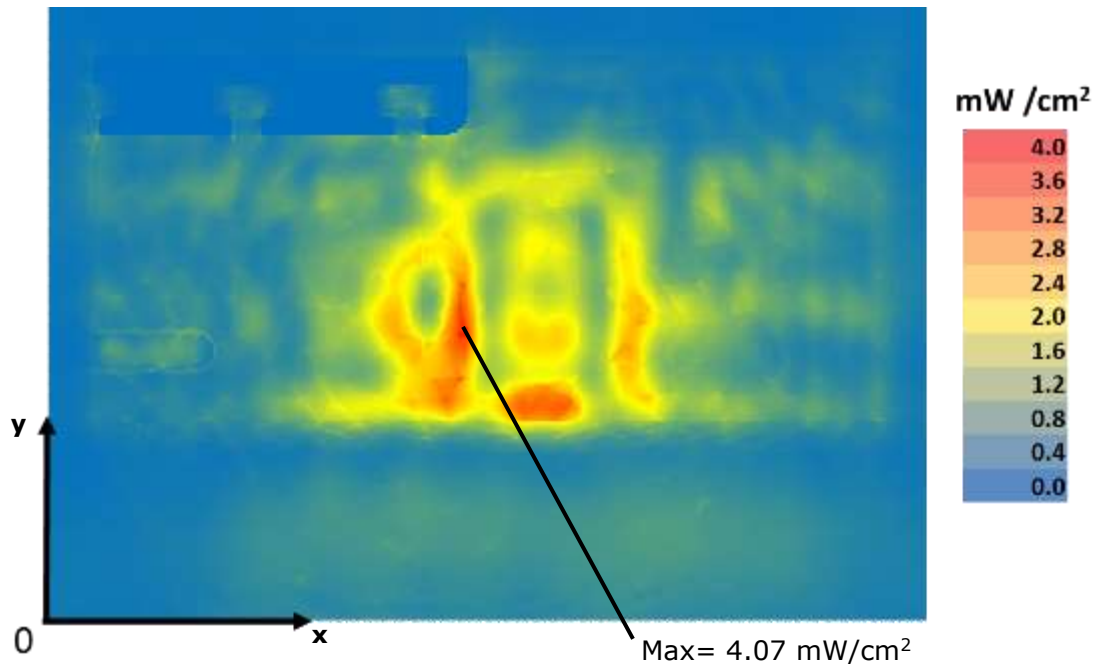


Figure 29 – Channel 1 upper bound, Single-point Power Density mesh on platform base

Worst case coordinate on channel 2 are X = 24.6 mm, Y = 15.7 mm.

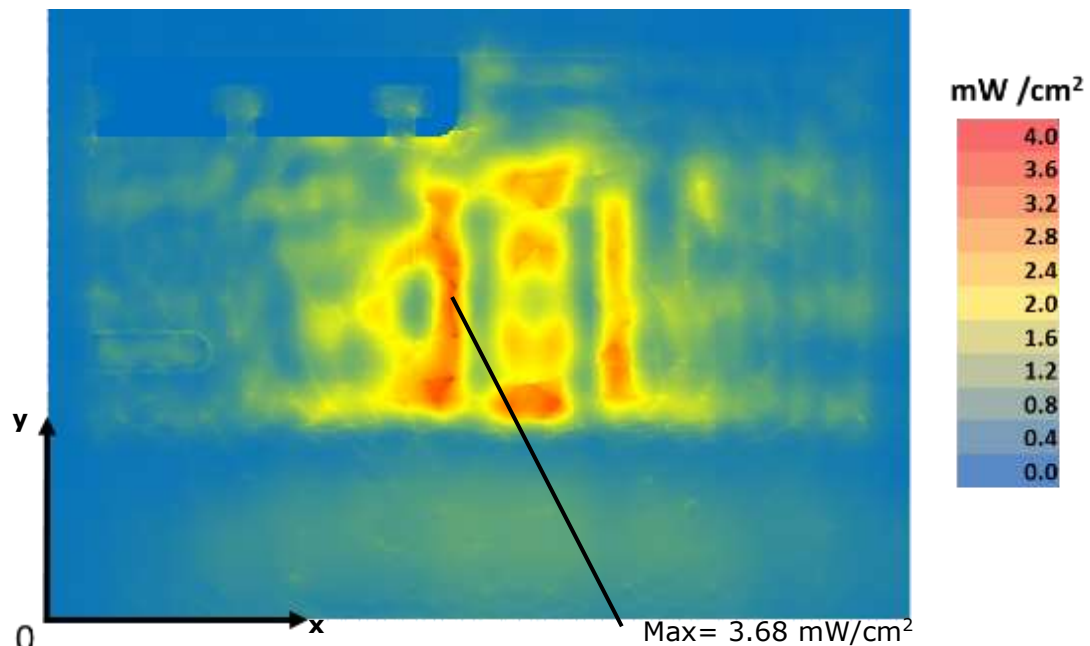


Figure 30 – Channel 2 upper bound, Single-point Power Density mesh on platform base

Worst case coordinate on channel 3 are X = 25.3 mm, Y = 19mm.

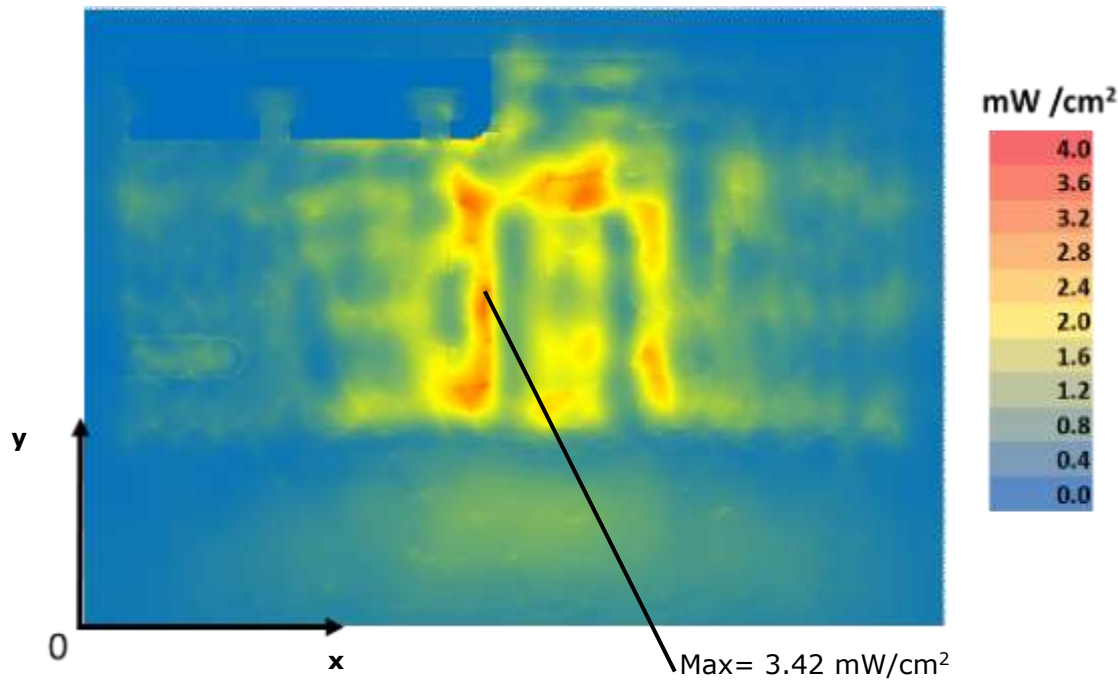


Figure 31 – Channel 3 upper bound, Single-point Power Density mesh on platform base

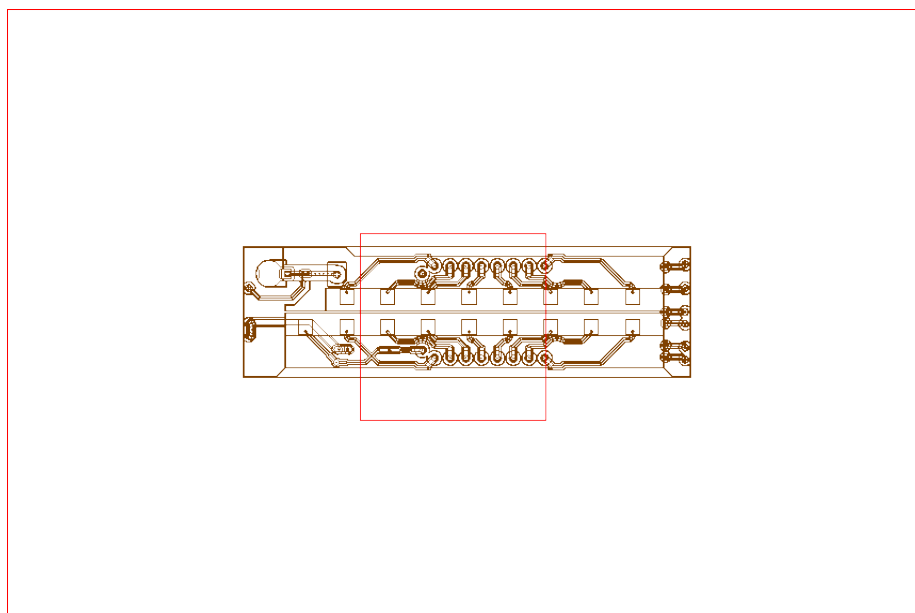


Figure 32 – Footprint of single-point power density plane representation in base plane



4.2.2 Single-point power density values with worst case antenna phases for base plane exposure

The Table 6 shows the phase for each antenna elements per channel for the worst case found as described in the chapter 3.4. The phases search algorithm is detailed in point 5 of the section 3.4.3.

| Antenna index | Phases [Degrees] | | |
|---------------|------------------|-----------|-----------|
| | Channel 1 | Channel 2 | Channel 3 |
| 0 | 180 | 225 | 270 |
| 1 | 270 | 315 | 0 |
| 2 | 0 | 45 | 90 |
| 3 | 180 | 180 | 225 |
| 4 | 135 | 180 | 270 |
| 5 | 225 | 270 | 315 |
| 6 | 315 | 0 | 45 |
| 7 | 135 | 180 | 225 |
| 8 | 0 | 45 | 45 |
| 9 | 90 | 135 | 135 |
| 10 | 225 | 225 | 225 |
| 11 | 0 | 0 | 0 |
| 12 | 270 | 0 | 45 |
| 13 | 45 | 90 | 135 |
| 14 | 180 | 180 | 225 |
| 15 | 0 | 0 | 0 |

Table 6 – Phases configurations for the worst case

The amplitude on each antenna is -6dBm as explained in chapter 3.6.

The Figure 33, Figure 34 and Figure 35 present power density in the body direction using worst case antenna phases presented in the Table 6. The simulated power density area has a size of is 49.5 mm x 32.4 mm, this area corresponds to the blue delimitation. The footprint of the platform components is showed directly in the figures.

Table 7 presents the ratios (linear and logarithmic) at the highest single-point value for the Z trajectory on the base area between the power density worst case value along the body direction (S_z) and the



Simulation Results

power density worst case value along the propagation direction (S_{tot}) for all channels and taking into account all components. This table confirms that the power density component along Z is the principal contributor in the total power density. Also the ratios are used for results scaling in Table 9 of section 4.2.5 and in the compliance summary discussion in section 6 .

| BASE AREA | Channel 1 | Channel 2 | Channel 3 |
|--|-----------|-----------|-----------|
| Mag S_{tot} (maximum poynting single-point value with all components) [mW/cm ²] | 2.384 | 2.146 | 2.253 |
| S_z (trajectory of the above on Z direction) [mW/cm ²] | 2.357 | 2.098 | 2.166 |
| Ratio (S_z / S_{tot}) (linear) | 0.988 | 0.977 | 0.961 |
| Ratio $10\log(S_z / S_{tot})$ (dB) | -0.05 | -0.1 | -0.17 |

Table 7 – Ratios between Z-power density and total power density on base area

Please note that in the top left of each figure there is an area with ~0 energy, this is explained by the fact that there is metal in this place in the platform and is an expected result

Worst case coordinate on channel 1 are X = 24 mm, Y = 15.4 mm.

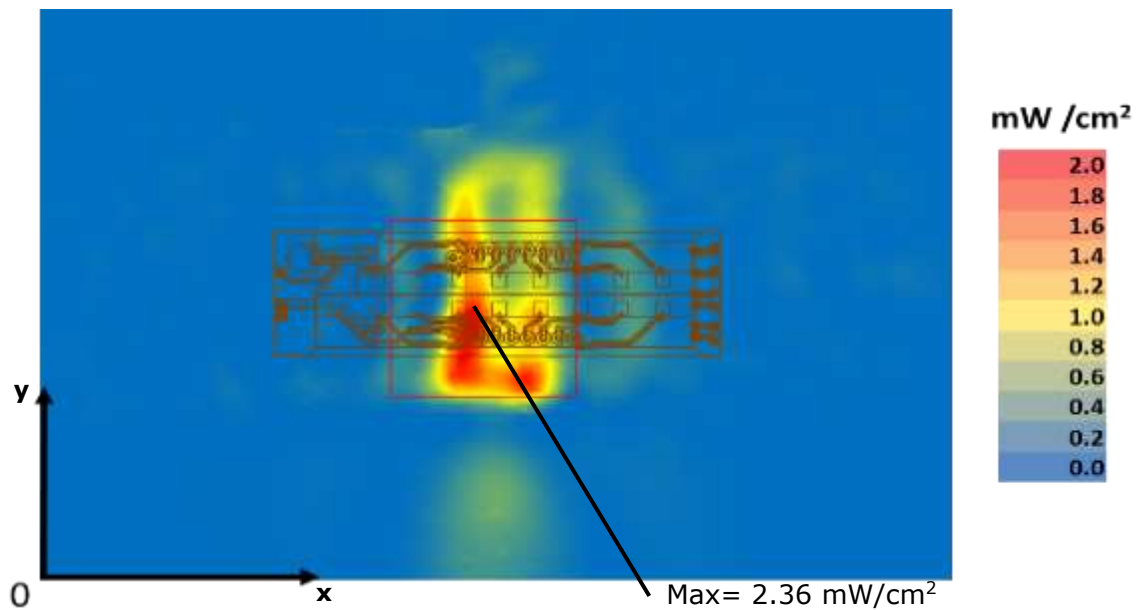


Figure 33 – Channel 1 single-point power density mesh on platform base

Worst case coordinate on channel 2 are X = 26.6 mm, Y = 16.2 mm

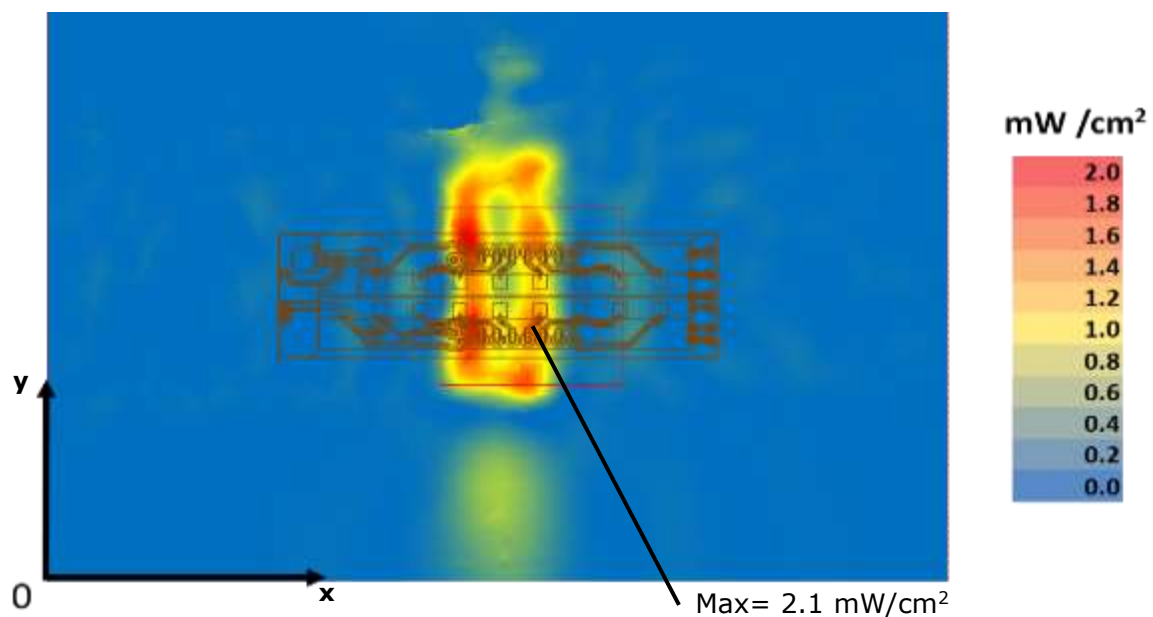


Figure 34 – Channel 2 single-point power density mesh on platform base

Worst case coordinate on channel 3 are X = 27mm, Y = 19.8 mm.

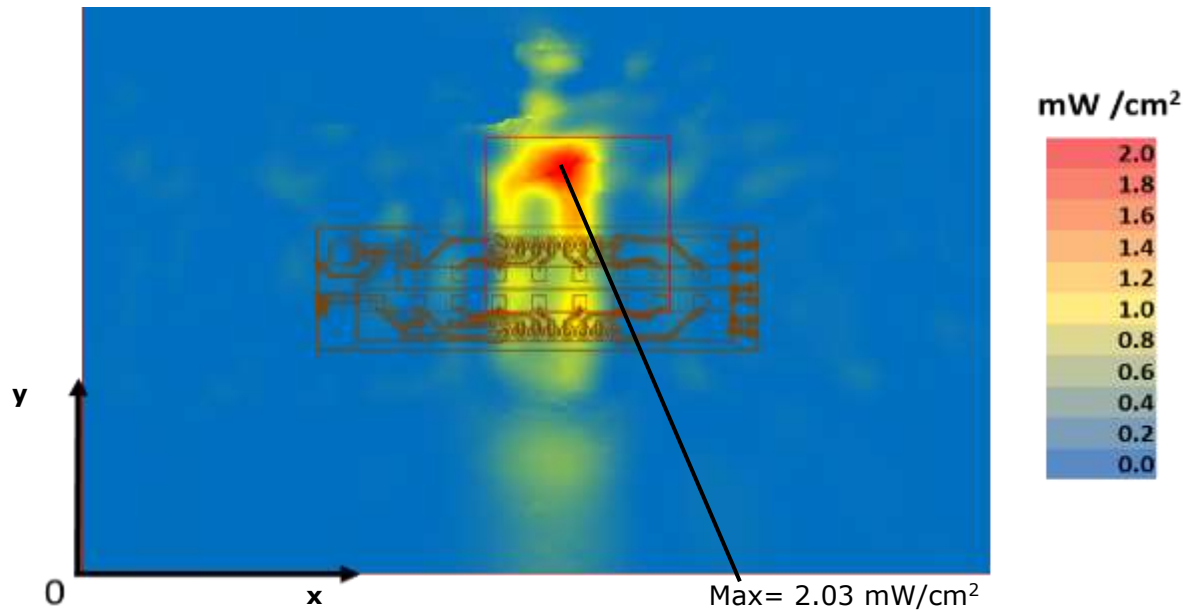


Figure 35 – Channel 3 single-point power density mesh on platform base

The highest value shown in these figures is a point and not yet integrated over the 1cm^2 . The final power density value is given in section 4.2.5.

4.2.3 One dimensional cut of the mesh single-point power density for base plane exposure

In Figure 36 – Figure 38 below, we present a subset of the simulation results from the Z component single-point power density values with worst antenna phases (chapter 4.2.2).

The subset is a 1 dimensional cut in the X axis and Y axis that shows the behavior of the near field power density at zero distance.

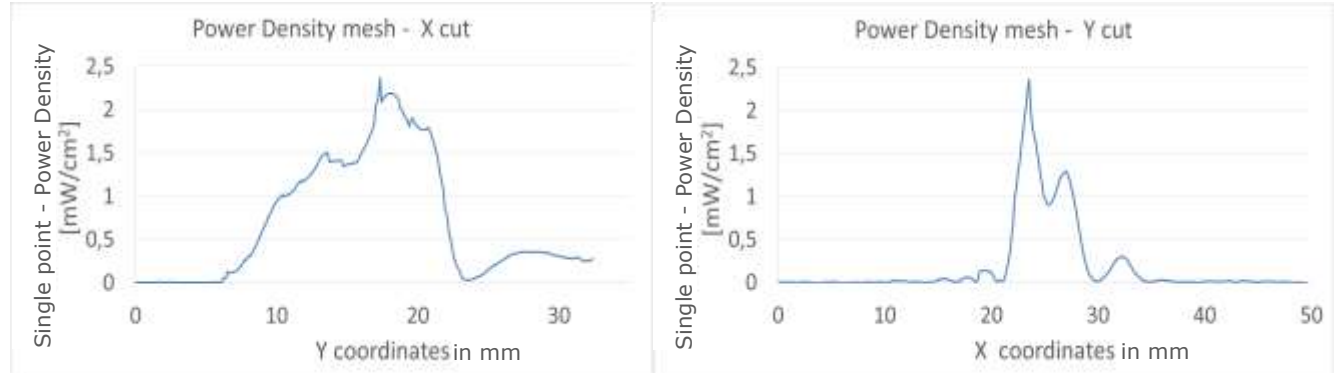


Figure 36 – One dimensional plots of the power density on Channel 1

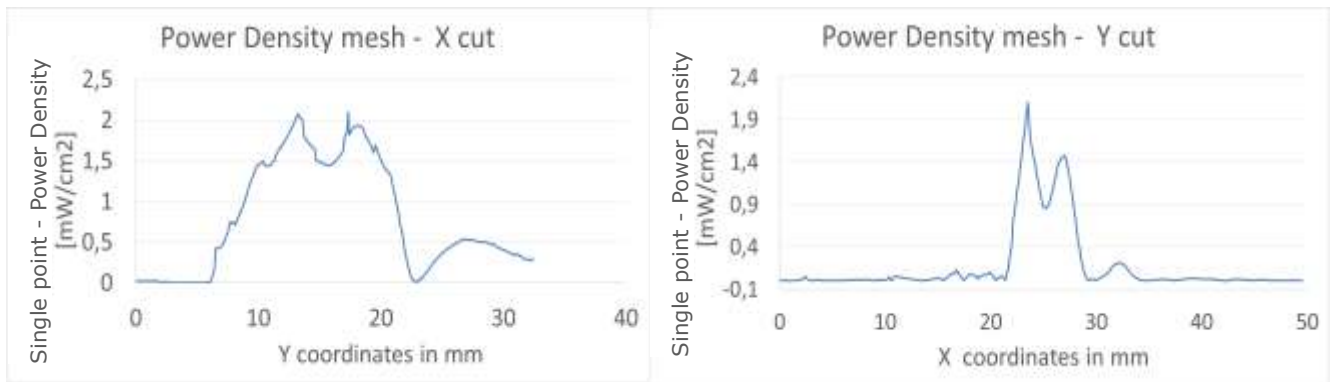


Figure 37 – One dimensional plots of the power density on Channel 2

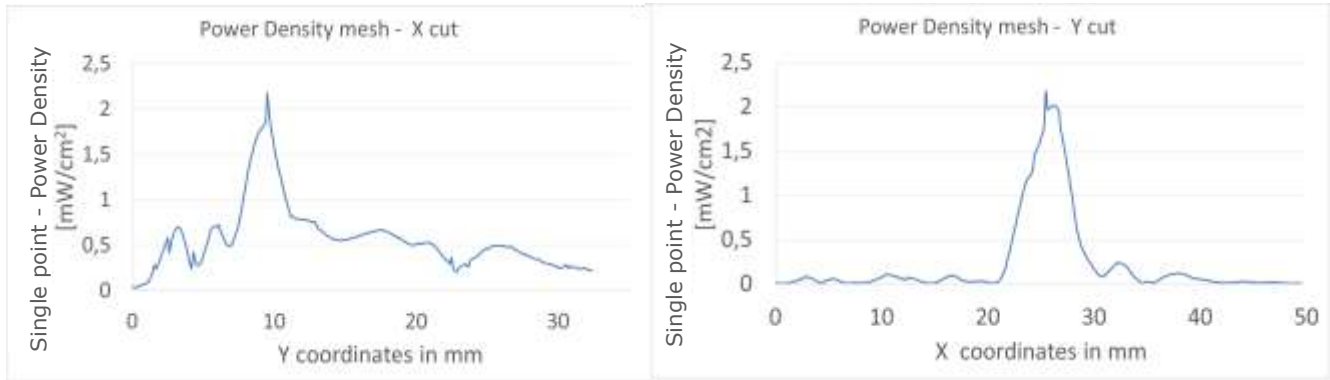


Figure 38 – One dimensional plots of the power density on Channel 3

4.2.4 Integrated power density over 1 cm² for base plane exposure

Figure 39 – Figure 41 below present the Z-integrated power over 1cm² at 100% duty cycle for the worst case scenario as explained in section 3.4.3. The plane dimensions of these results is 39.5 mm x 22.4 mm. The footprint of the platform components is showed directly in the figures.

The 1cm² square location correspondent to the maximum of integrated power density value for each channel is plotted in red in figures below (Figure 39 – Figure 41). The maximum average values are mentioned in the second row of Table 8. The worst case coordinates are the center of the squares.

Worst case coordinate on channel are X = 19 mm, Y = 10.4 mm.

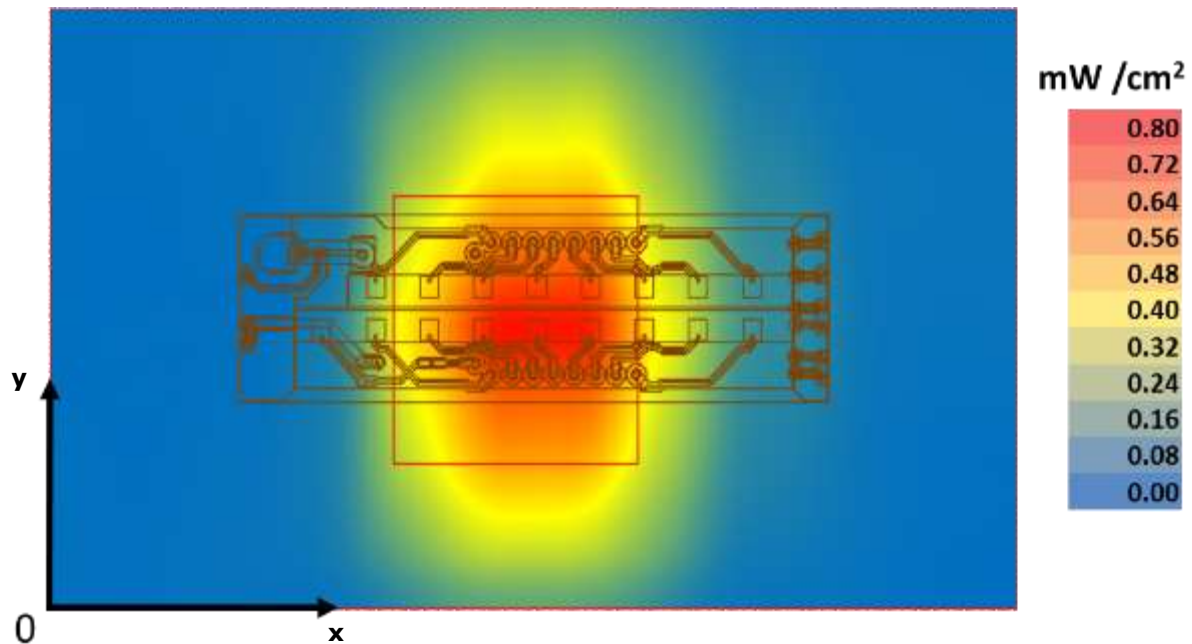


Figure 39 – Channel 1 worst case - Integrated power over 1cm² on platform base

Worst case coordinate on channel 2 are X = 21.6 mm, Y = 11.2 mm.

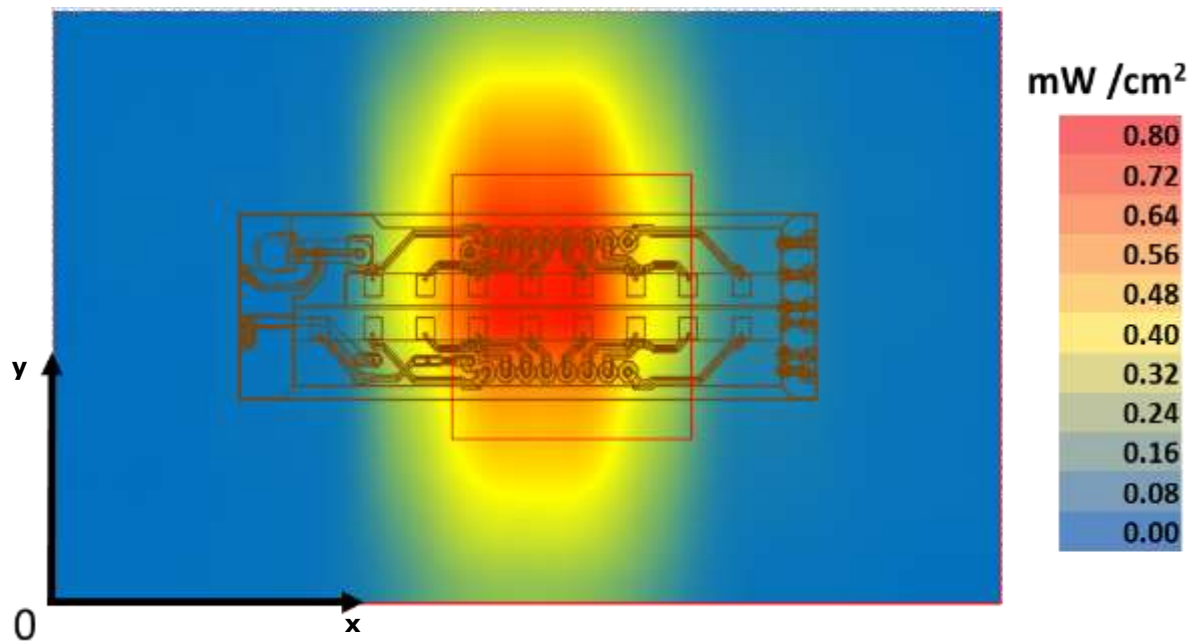


Figure 40 – Channel 2 worst case - Integrated power over 1cm² on platform base

Worst case coordinate on channel 3 are X = 22 mm, Y = 14.8 mm.

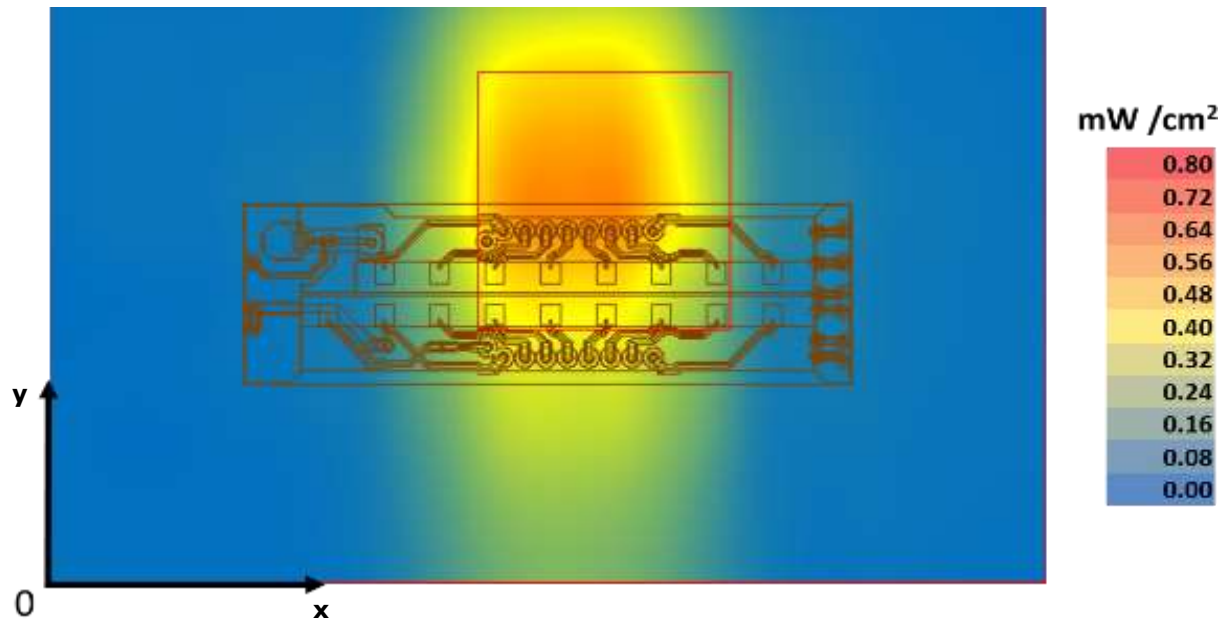


Figure 41 – Channel 3 Worst case - Integrated power over 1cm² on platform base

4.2.5 Power density for base plane exposure

The Figure 42, Figure 43 and Figure 44 show the worst case power-density integrated over 1cm^2 versus the distance. As described in section 3.4.3 and section 3.5.2 the worst case was computed by the simulation using the worst case antenna phases and the worst platform configuration (Tablet mode). The 0mm reference correspond to the platform boundary, the active antenna located inside the platform is at 13.9 mm from this distance.

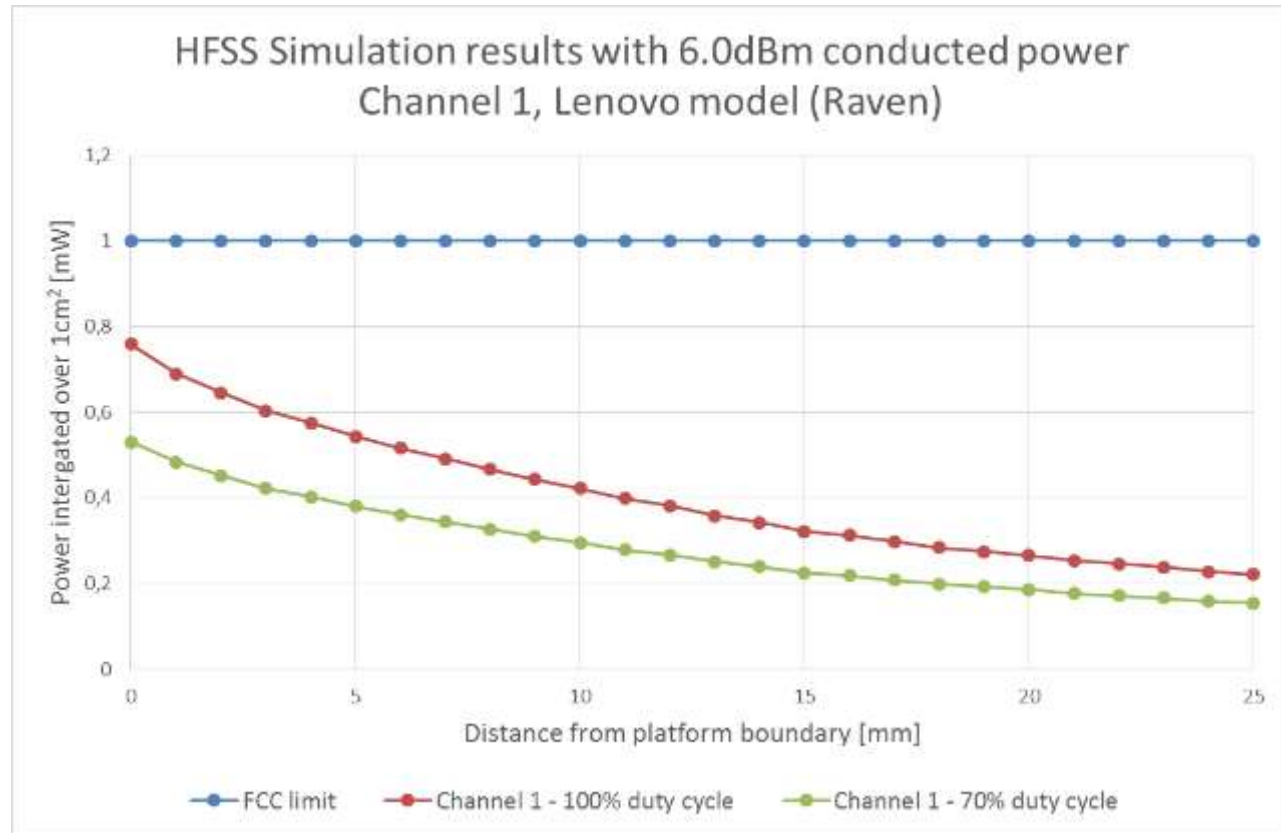


Figure 42 – HFSS Simulation results in Ch1 (Base Plane)

HFSS Simulation results with 6.0dBm conducted power
Channel 2, Lenovo model (Raven)

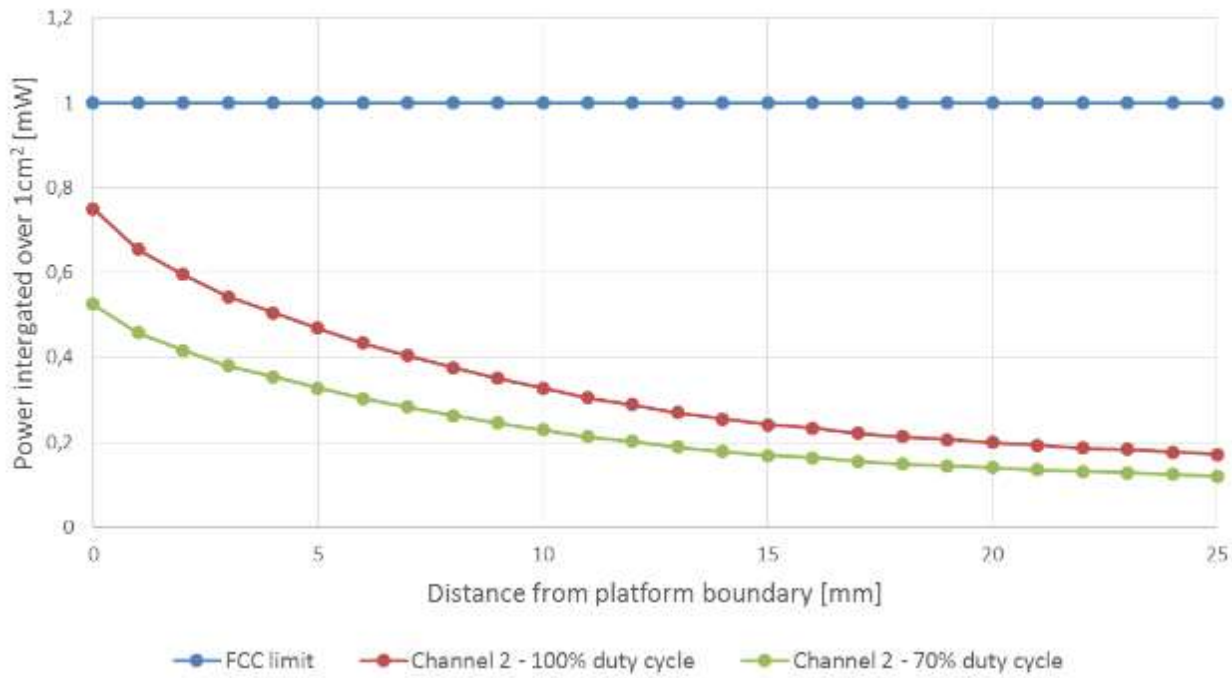


Figure 43 – HFSS Simulation results in Ch2 (Base Plane)

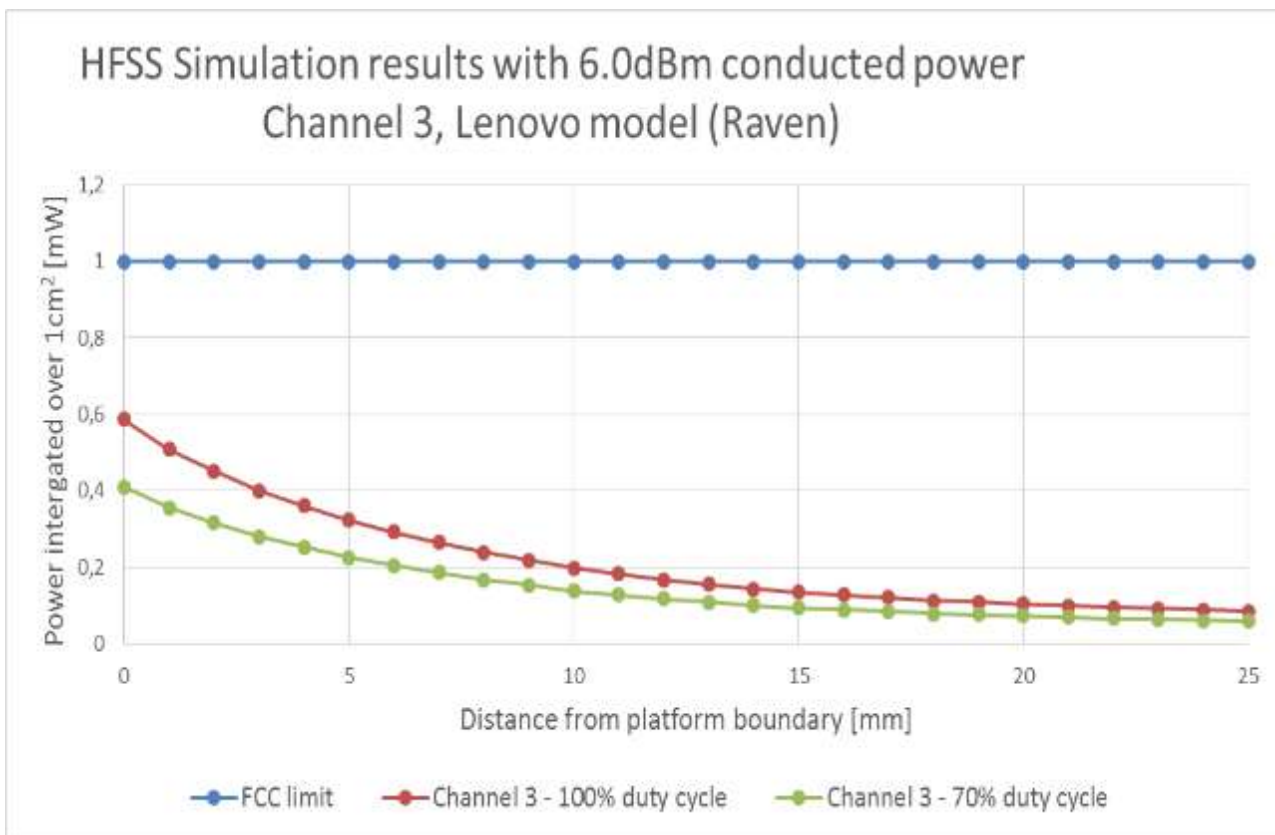


Figure 44 – HFSS Simulation results in Ch3 (Base Plane)

The Table 8 shows the simulated worst case power density at the base plane area for each channels.

| Base plane Highest power density | Channel 1 [mW/cm ²] | Channel 2 [mW/cm ²] | Channel 3 [mW/cm ²] |
|-------------------------------------|------------------------------------|------------------------------------|------------------------------------|
| 70% duty cycle | 0.531 | 0.525 | 0.411 |
| 100% duty cycle | 0.759 | 0.750 | 0.587 |

Table 8 – Worst case power density - Base plane



Notes for Table 8:

1. The worst case channel is channel 1.
2. The Maximum power density (spatially integrated over worst 1cm²) in channel 1 (worst case) is achieved at 0mm distance from the platform boundary and equals to 0.759 mW/cm² over 100% duty cycle.
3. As explained in section 2.3, the Intel 18260NGW module is limited to transmit at a duty cycle of 70% over 10sec. Therefore the maximum spatially integrated and time averaged power density over 1cm² is $0.759 \times 0.7 = 0.531$ mW/cm².
4. Taking into account the ratios presented in Table 7 between the Z-component and the total power density, the integrated power densities values at zero distances become:

| | Channel 1 | Channel 2 | Channel 3 |
|---|------------------|------------------|------------------|
| Integrated Power density in Z-direction (P_z) [mW/cm²] | 0.531 | 0.525 | 0.411 |
| Corresponding Ratio (R) | 0.988 | 0.977 | 0.961 |
| Global Integrated Power density ($P_{tot}=P_z/R$) [mW/cm²] | 0.537 | 0.537 | 0.427 |

Table 9 – Base plane integrated power density at zero distance

Therefore, the worst case channel remains channel 1 and the maximum spatially integrated and time averaged total power density over 1cm² is $0.531 / 0.988 = 0.537$ mW/cm².

4.3 Conclusion

The simulation results over 2 planes were presented in this report, the simulation on the edge of the platform and the base of the platform are described in the section 3.5.3. The worst case has been shown for the base plane using channel 1 in the Z direction with the maximum power density is 0.531 mW/cm², and for the edge plane using the channel 2 with three components, the maximum power density is 0.747 mW/cm². Note that the applicable FCC limit is 1 mW/cm².

5 Validation of Simulation Model in Transition-Zone Field to Far-Field

Due to the lack of standardized code validation, benchmarking and uncertainty estimations of the simulation software and the implemented device geometry, the near field to far field measurement results are included for the purpose of providing confidence for the software simulation model used and that the results produced were within an acceptable range when compared with the measured results. The error margins of all test results are requested to be considered collectively by the FCC to determine compliance.

To validate the accuracy of the simulation we took a few metrics, presented in this chapter, including correlation of the simulated power density in transition-zone field to far-field against lab measurements. The same simulation was used for both power density estimation in near field (previous chapter) and transition-zone field to far field correlation (this chapter).

5.1 Correlation of E.I.R.P. in the near to far field

Note – the correlation of E.I.R.P. in transition field to far field was done with conducted output power of 6dBm. This value was used for both lab measurements and simulation results.

5.1.1 Far field boundary calculation

Far field boundary can be estimated using *Fraunhofer distance* equation:

$$\text{Far FieldBoundary} = \frac{2d^2}{\lambda}$$

Equation 2 – Far field boundary calculation

In the RFEM 2, d (largest antenna dimension) = 16.15mm (see Figure below)

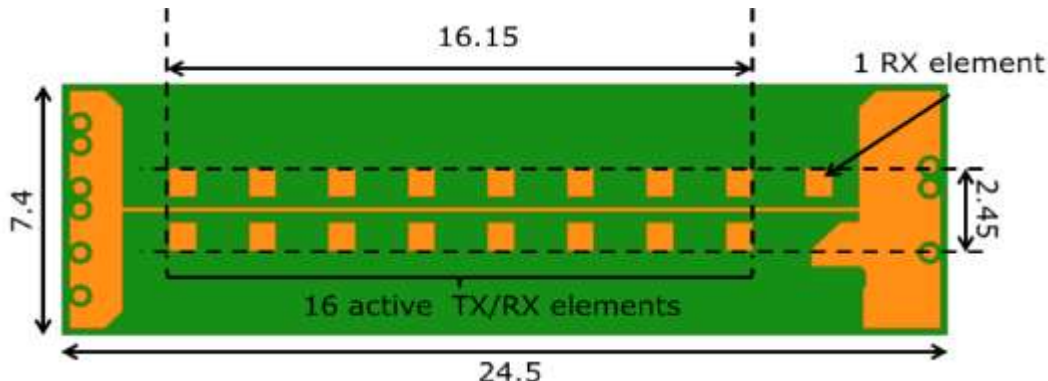


Figure 45 – Antenna Dimensions in mm

| Channel | λ (wave length) [mm] | Fraunhofer distance [cm] |
|---------|------------------------------|--------------------------|
| 1 | 5.14 | 10.1 |
| 2 | 4.96 | 10.5 |
| 3 | 4.79 | 10.8 |

5.1.2 Test laboratory

The measurements were done at the ISO 17025 accredited laboratory Intel Mobile Communications France S.A.S. with FCC registration number #3478.01 on Lenovo Model TP00076B platform with 18260NGW module. Data can be found in the test report 160205-04.TR01, submitted with the application for this FCC ID.

5.1.3 Correlation of measurements and simulation

The figure in this section show E.I.R.P comparison simulation and measurements. The measured E.I.R.P. values from the test report 160205-04.TR01 are normalized to 100% duty cycle.

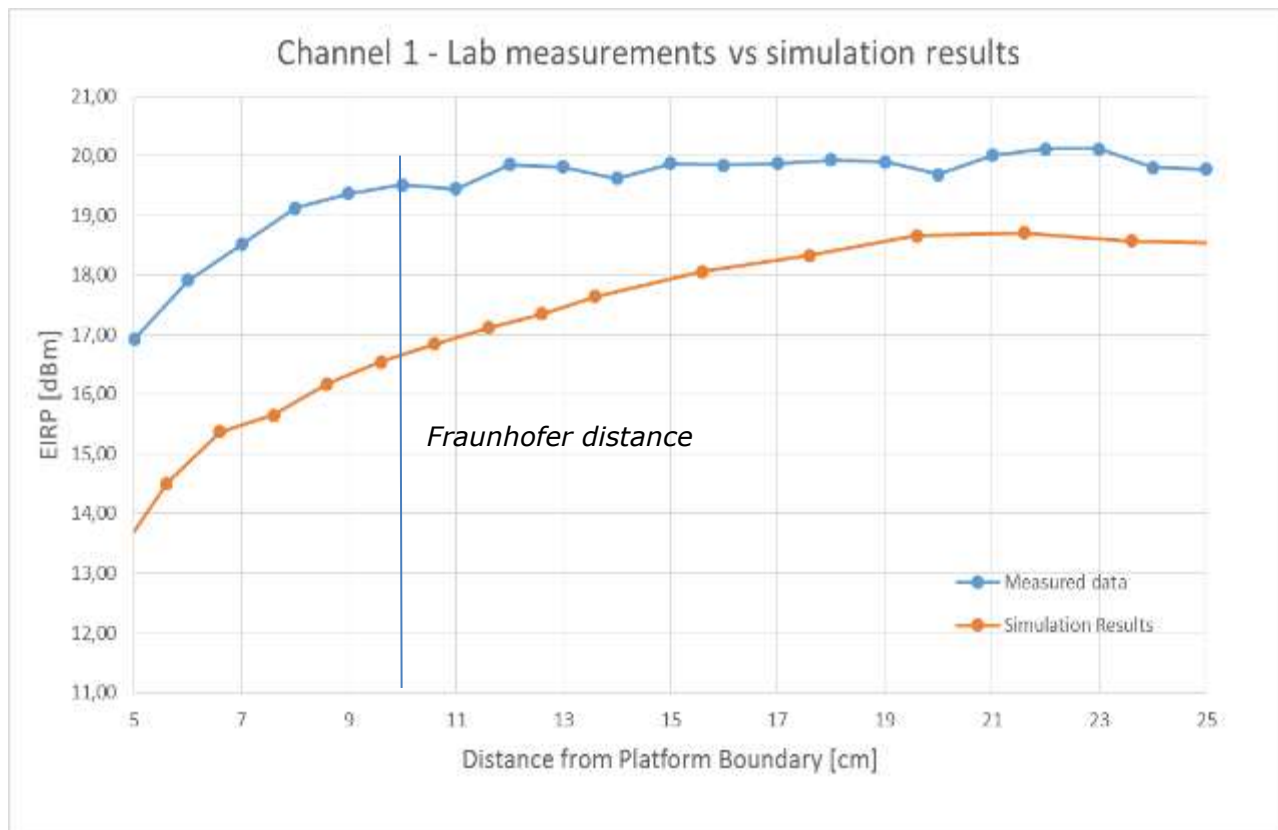


Figure 46 – Comparison of E.I.R.P. simulation to lab measurements – channel 1

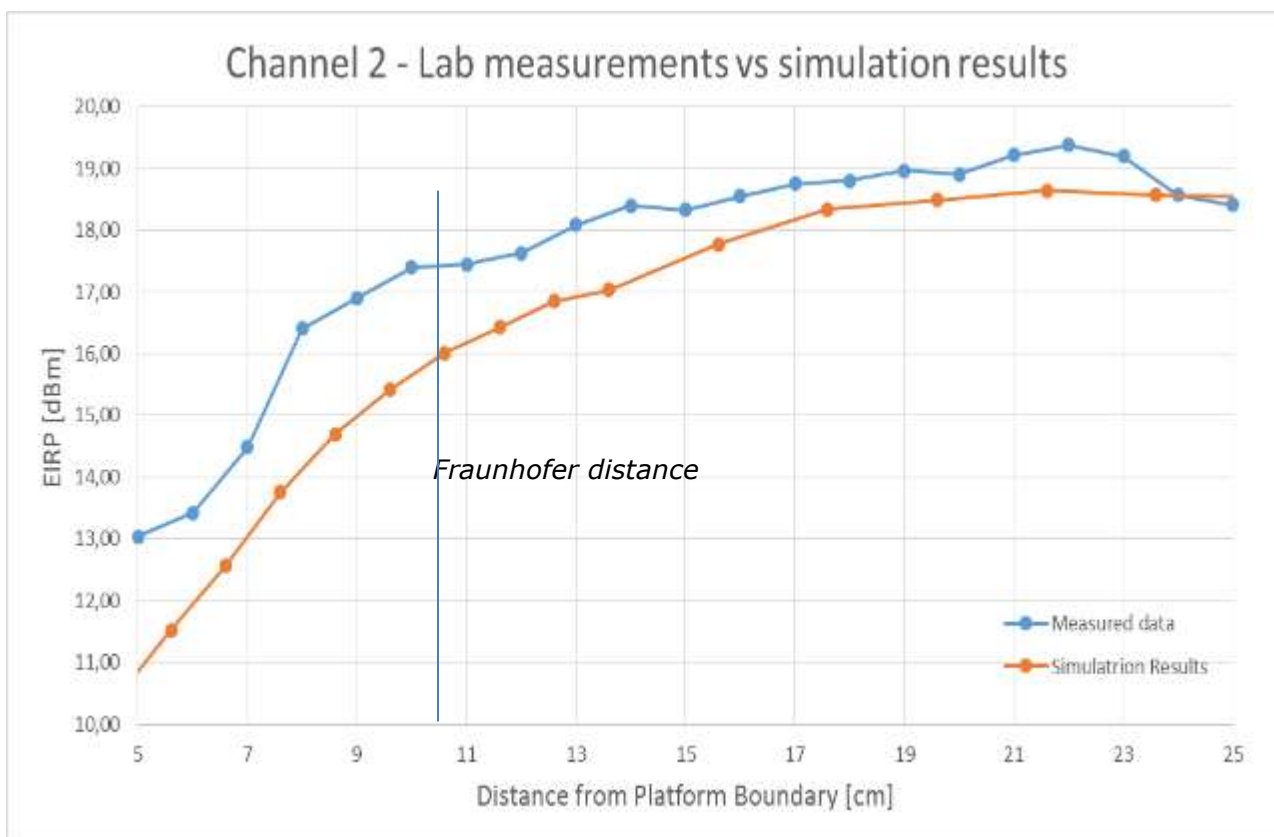


Figure 47 – Comparison of E.I.R.P. simulation to lab measurements – channel 2

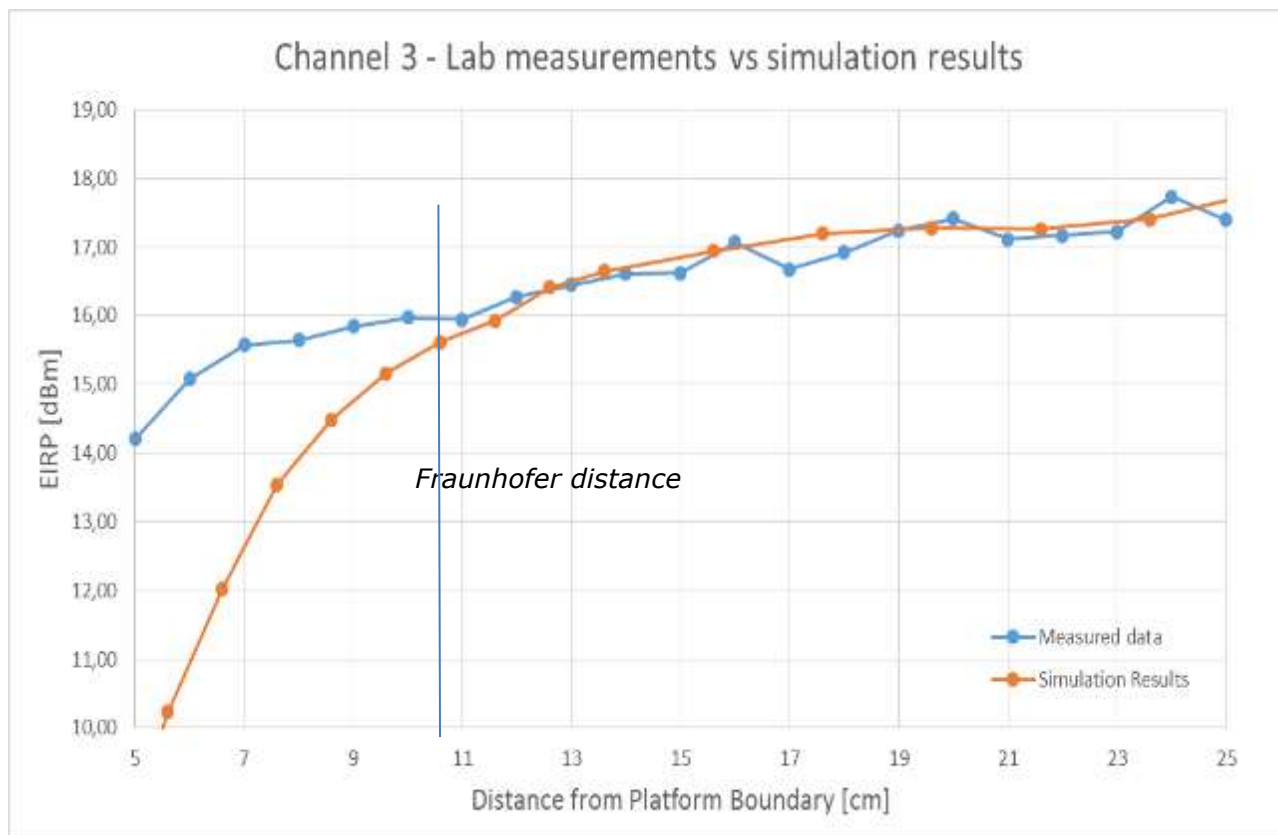


Figure 48 – Comparison of E.I.R.P. simulation to lab measurements – channel 3

The following observations can be made by looking at Figure 46 - Figure 48:

1. Measured E.I.R.P. increased to a steady state, demonstrating we are in the transition-zone field below 10cm (very close to the Fraunhofer distance).
2. Good correlation can be seen in steady state power, with up to ~ 1 dB difference between measured power and the simulated power.
3. Some difference can be seen in the energy build up between simulation results to lab measurements. This difference is probably due to near field effect and coupling between the platform to the antenna that is used for the measurements.

5.1.4 Estimated conducted power level

Measured E.I.R.P. signal power can be used to estimate the equivalent conducted power that is fed to the antenna array. The estimation is done by subtracting the antenna gain from the estimated E.I.R.P. level.

The E.I.R.P. level is the same as reported in previous section while the antenna gain is the antenna gain that is used in the 18260NGW modular approval.

Free space antenna gain: Channel 1 – 15.30dBi, Channel 2 – 15.20dBi, Channel 3 – 14.8dBi

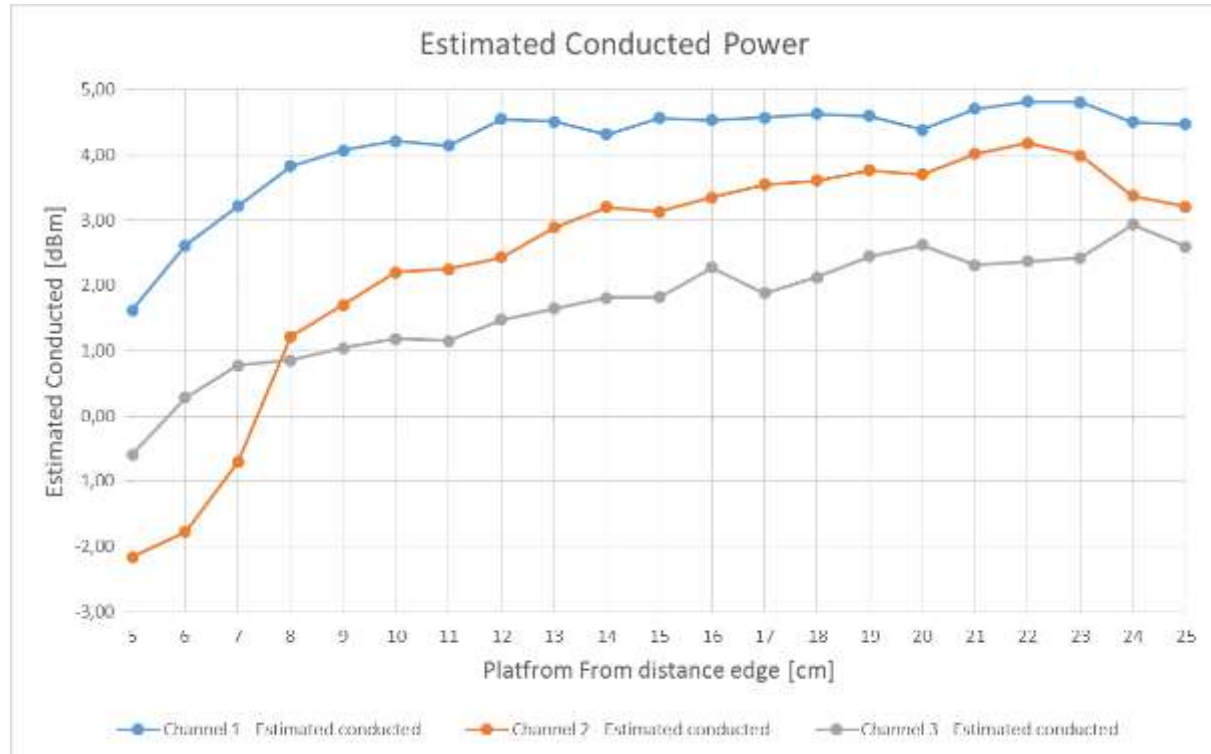


Figure 49 – Estimate conducted power from E.I.R.P. data

Looking at Figure 49 one can see that the estimated conducted power is lower than the actual power level that was used. The tests were done with a conducted power of 6dBm while the estimated for channels 1 is ~4.5 dBm, channel 2 ~3.5 dBm & channel 3 ~2 dBm

1. The antenna gain that is used for this estimation is the modular antenna gain (antenna in free air). However the antenna that is embedded inside a platform has a platform loss that is typically in the vicinity of 1.5dB to 3.0dB. This additional platform loss explains the power that is estimated for channels 1, 2 & 3.
2. Lower estimated conducted power can be seen at short distances (up to about 15 cm) as coupling with the measuring device or other near objects. In addition at this range (4-10 cm) the antenna gain is lower than the far field antenna gain, hence E.I.R.P. is lower and the predicted power is lower.

5.2 Simulating a canonical antenna design

A simple patch antenna with Length = 7.5mm (GND plane length), and Lambda = 4.8mm, and was designed to work at 62.5GHz, as can be seen in the figure below.

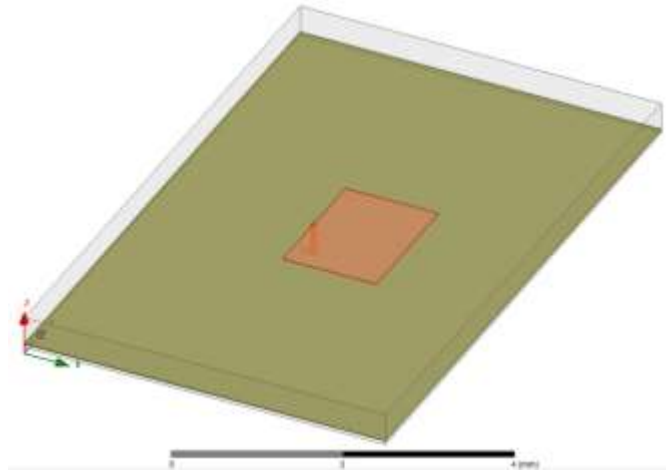


Figure 50 – Simulation of a single Patch antenna

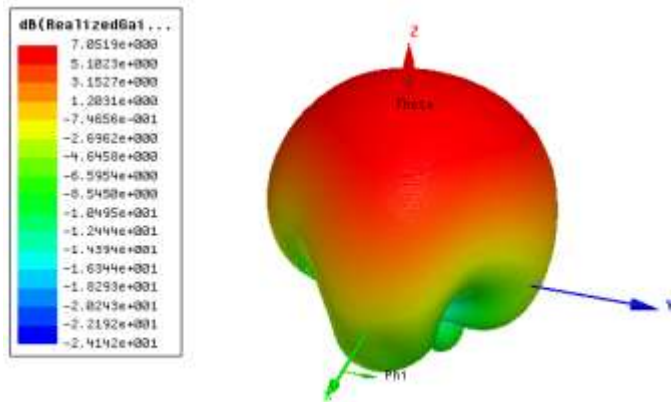


Figure 51 – Patch Antenna Gain

The simulated Far-Field Max Realized Gain [dBi] is 7.05[dBi], as simulated by far field simulation. The 7.05dBi gain was obtained using HFSS simulation using Far Field Gain option.

Theoretically patch antenna gives \sim 7-9 dBi gain. The simulated patch antenna in the HFSS simulation is not a theoretical patch, it includes several “real life” non-idealities (width, size, feeding point etc). The 7.05 dBi Max Realized Gain is the gain obtained from HFSS simulation including those non-idealities.



Validation of Simulation Model in Transition-Zone Field to Far-Field

A few test planes were integrated into the simulation at different far-field distances from the patch (shown below) for power density calculations:

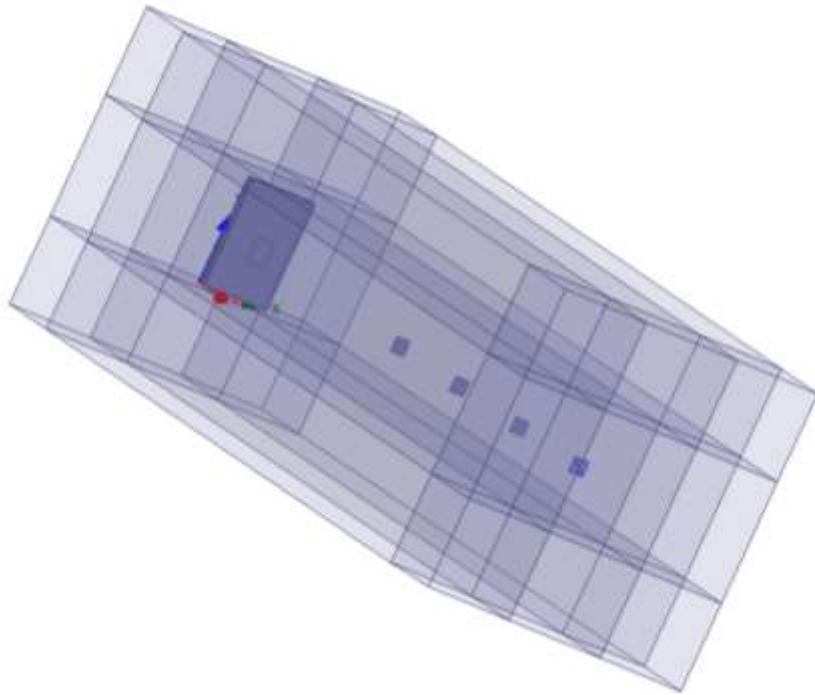


Figure 52 – Simulation 3D structure

The distances between the patch and the test planes range from 24mm to 54mm.

To validate the numerical tool, the power density results at the test planes are translated into gain using omnidirectional power propagation and compared to far field gain according to simulation (table below).

The table below summarizes the results:

| Far Field Distance | $P_{omni} = \frac{P}{4\pi R^2} \left[\frac{W}{mm^2} \right]$ | Power Density from simulation $\left[\frac{W}{mm^2} \right]$ | Gain calculation from power density [dBi] |
|--------------------|---|---|---|
| 24mm | 1.34e-4 | 6.70e-4 | 6.99 |
| 29mm | 9.11e-5 | 4.61e-4 | 7.04 |
| 34mm | 6.59e-5 | 3.38e-4 | 7.10 |
| 44mm | 3.91e-5 | 2.03e-4 | 7.15 |
| 54mm | 2.59e-5 | 1.35e-4 | 7.17 |

Table 10 – Gain calculation from power density per several distances

Where P is the simulated radiated power and R is the distance from the patch to the test plane.



The table above shows excellent correlation between the Patch antenna gain calculated from power density, to the Far-Field Max realized gain (7.05[dBi]). This is also depicted in the figure below:

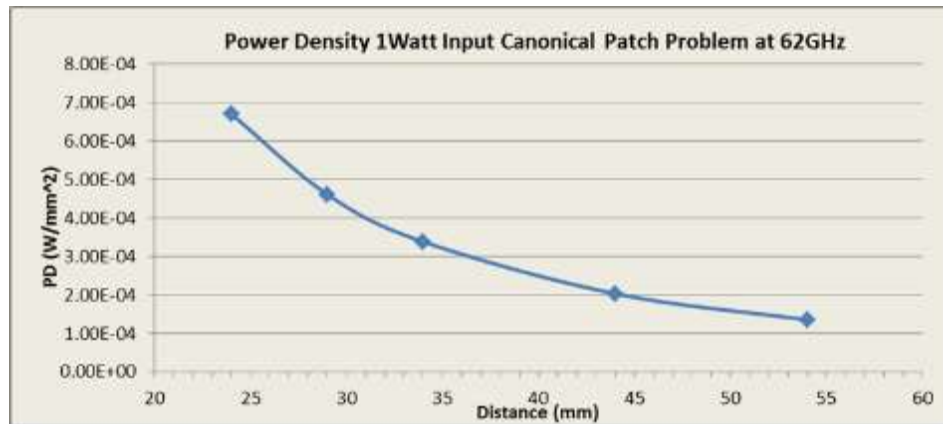


Figure 53 – Power Density of Canonical Patch Antenna



6 Summary

Due to the lack of standardized code validation, benchmarking and uncertainty of the simulation software, the near field to far field results are included for the purpose of providing confidence for the software simulation model used and that the results produced were within an acceptable range when compared with the measured results. The error margins of all test results have been considered collectively by the FCC to establish confidence for the accuracy of the HFSS simulation.

Per consultation with FCC staff, it is accepted to use the adjustment of power density based on differences between the normal component of the Poynting vector and 3 components Poynting vector using the simulation results for the worst case antenna configurations for this specific filing and circumstances only.

The following table summarizes the simulation results in the near field of Intel 18260NGW module, embedded in Lenovo Model TP00076B:

| Parameter | Value |
|---|--------------------------|
| Total conducted power | 6.0 dBm |
| Maximum TX duty-cycle | 70% |
| Maximum spatially integrated and timed average power density, over 1cm ² and 10 seconds (CH1 Base plane) | 0.531 mW/cm ² |
| Maximum spatially integrated and timed average power density, over 1cm ² and 10 seconds taking into account the ratios presented in Table 3,6 (CH2 – Edge plane) | 0.747 mW/cm ² |

Table 11 – Summary of simulation results for RF exposure compliance

Therefore Intel 18260NGW module, embedded in Lenovo Model TP00076B, complies with FCC rule parts §2.1093 and §15.255(g).